Electrocatalytic Activity of Transition Metal Substituted Heteropolytungstates

Thesis by

James E. Toth

In Partial Fulfillment of the Requirements

for the Degree of

Doctor of Philosophy

California Institute of Technology

Pasadena, California

1990

(Submitted August 10, 1989)

Acknowledgments

I would like to thank my advisor, Fred Anson, for his kind support over the last four years. Working in his group been a tremendous learning experience, one that will influence me throughout my scientific career. I would also like to thank the chairman of my committee, Harry Gray, for his encouragement and his interest in my work. I would especially like to thank the people that were at Allied-Signal who convinced me to return to grad school. I would have never started this adventure without the encouragement of Jane Frommer, Jim Wolf, and Larry Shacklette.

Many members of the Anson group, past and present, have given me helpful comments about the work contained in this thesis, but I would especially like to thank Paul Bernhard, Jody Redepenning, and Dave Malerba as well as John Brewer of Harry's group for their helpful suggestions. The ion chromatography that is discussed in Chapter 4 could not have been performed without the aid of Bill Munger of the Caltech environmental engineering department. Bruce Tufts was kind enough to run XPS experiments on the ruthenium substituted ions and I must thank Dave Wheeler for running nmr spectra of every bizarre nucleus I could think of, as well as making sure I got my money's worth out of my Atheneum dues.

Very special thanks go to my family for their continued support over the course of this work. I would also like to acknowledge B. P. of America for a graduate fellowship.

Finally I would like to thank all the crazy people that I have met here at Caltech, who have in turn kept me sane. The most memorable experiences of the last four years will no doubt be the fun and games enjoyed with people such as LeRoy Whinnery, Dave Wheeler, John and Cathy Cox, Dave Shuey, Jeff Stack, and especially Thu Le.

ABSTRACT

The electrochemical and electrocatalytic behavior of a series of heteropolytungstate anions in which a tungsten atom in the well known Keggin structure has been replaced by an iron atom is described. All of the iron substituted ions exhibit a one electron reversible couple associated with the Fe^{3+} center and a pair of two electron waves attributed to electron addition and removal from the tungsten oxo framework. The pH and ionic strength effects upon the various electrochemical processes are discussed and interpreted in terms of a competition between protonation and ion pairing of the highly negatively charged ions.

The anions are efficient catalysts for the electroreduction of hydrogen peroxide. A catalytic mechanism involving a formally Fe(IV) intermediate is proposed. Pulse radiolysis experiments were employed to detect the intermediate and evaluate the rate constants for the reactions in which it is formed and decomposed. A chain mechanism for the catalytic decomposition of hydrogen peroxide in which the Fe center shuttles between the +2, +3, and +4 oxidation states is proposed to explain the non-integral stoichiometry observed for the iron substituted polytungstate catalyzed electroreduction of hydrogen peroxide.

The anions are also efficient electrocatalyst for the electrochemical conversion of nitric oxide to ammonia. The catalyzed reduction does not produce hydroxylamine as an intermediate and

appears to depend upon the ability of the multiply reduced heteropolytungstates to deliver several electrons to the bound NO group in a concerted step. A valuable feature of the heteropolytungstates is the ease at which the formal potentials of the several redox couples they exhibit may be shifted by changing the identity of the central heteroatom. Exploitation of this feature provided diagnostic information that was decisive in establishing the mechanism of electrocatalytic reduction.

The iron substituted heteropolytungstates are not degraded by repeated cycling between their oxidized and reduced states. They also show superior activity compared to their unsubstituted analogues, indicating that the Fe center acts as a binding site that facilitates inner-sphere electron transfer processes. The basic electrochemistry of several other transition metal substituted Keggin ions is also described.

TABLE OF CONTENTS

CHAPTER 1

INTRODUCTION

INTRODUCTION

The initial step in any electrocatalytic process usually involves the oxidation or reduction of a transition metal complex at an electrode surface. The oxidized or reduced complex can then diffuse into solution where it will react with another compound whose direct oxidation or reduction does not proceed at the electrode surface directly. This reaction returns the transition metal complex back to its original oxidation state, completing the catalytic cycle. Transition metal complexes are typically employed as catalysts because they have reversible electrochemical couples and can interact strongly with substrates through open coordination sites. Unfortunately, most transition metal complexes are only capable of transferring single electrons, that lead to the formation of high-energy radical intermediates afte electron transfer to the substrate. Electrocatalysts based on transition metal complexes with organic ligands, *e.g.*, porphines and other macrocyclic amines, are often susceptible to degradation in catalytic activity as a result of oxidation of the ligands by these high energy intermediates. With the hope of developing more robust electrocatalysts, we began examining the electrochemical and electrocatalytic behavior of a series of entirely inorganic, transition metal-substituted polyoxoanions. The initial compounds that we studied are derivatives of the heteropolytungstate anions known as Keggin ions (1). These compounds have the general formula $XW_{12}O_{40}^{m-}$ where X is a heteroatom such as Si, P, Ge or As, which is located at the center of a tetrahedron whose

apices are attached to four interconnecting tungsten-oxo triads each containing 3 tungsten and 10 oxygen atoms (1) (see figure 1.1).

In 1966 Baker *et al.* reported the synthesis of a related series of anions ($MXW_{11}O_{39}^{n-}$) in which a new transition metal cation (M) replaced one of the tungsten cations and the single terminal oxo group bound to it (2). Since then, synthesis of the stable lacunary ions ($XW_{11}O_{39}^{n-}$) (3) and a vast number of transition metal substituted derivatives (*e.g.*, M = Fe (4), Co (5,6), Ni (6), Mn (7), Cu (7)) have been reported. In such species the tungsten oxo cage serves as a pentadentate, homoleptic ligand with five bridging oxide anions available for coordination (2-7). The sixth coordination site of the newly incorporated transition metal is typically occupied by a labile water molecule that can be substituted with other ligands (4,5). This site could also serve as an entry to inner-sphere electron transfer pathways that are inaccessible to the unsubstituted, $XW_{12}O_{40}^{m-}$ anions.

There are several reasons why the transition metal substituted heteropolytungstates would be expected to be interesting electrocatalysts: 1) As stated above, the transition metal substituted compounds contain sites on the periphery of the ion were conventional inner-sphere processes can occur. 2) Despite their entirely inorganic composition, some of these transition metal-substituted heteropolyanions have been shown to exhibit catalytic chemistry similar to traditional transition metal complexes (8-10). They were reported to bind oxygen at low temperature (8) and catalyze the epoxidation of olefins by oxygen atom donors in organic solvents (9).

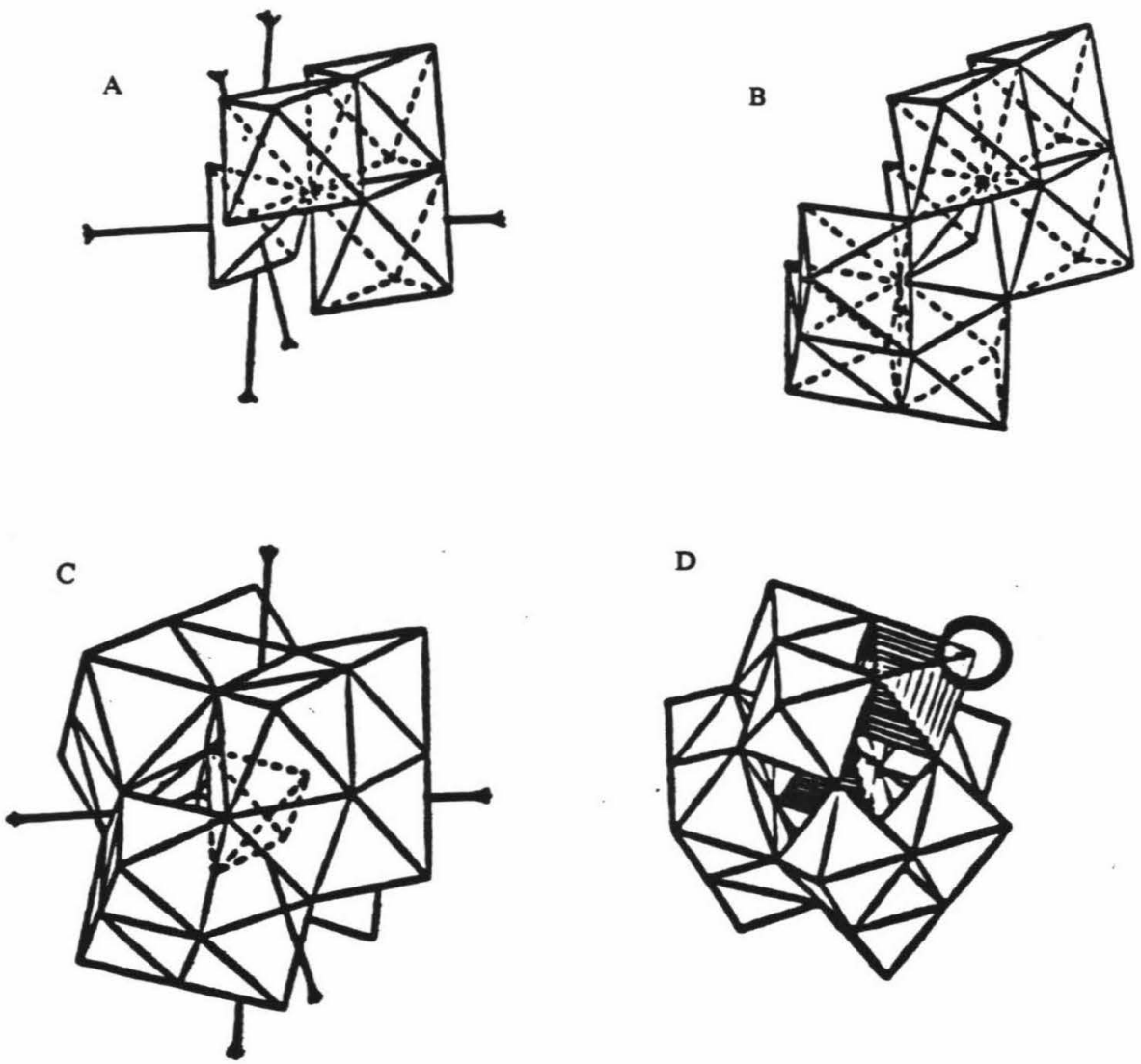

Figure 1.1: Schematic diagram of $XW_{12}O_{40}^{m-}$ (A-C) and $MXW_{11}O_{39}^{n-}$ (D) ions showing tetrahedral core and a single tungsten oxo triad (A), addition of second tungsten oxo triad (B), complete $XW_{12}O_{40}^{m-}$ ion (C), and site of transition metal substitution(D).

In fact, they have been referred to as inorganic porphyrins (8,10). 3) The ions are capable of being reversibly reduced by up to 5 electrons that could facilitate catalysis of multiple electron redox processes. 4) The compounds are relatively simple to synthesize and a large number of transition metals could be incorporated into the tungsten oxo framework(2-7). 5) A final desirable feature of the transition metal-substituted heteropolyanions is the ability to adjust the potential where the transition metal center exhibits its redox activity over a wide range by altering the identity of the heteroatom that is located in the center of the tungsten-oxide framework (7,11). Although this heteroatom is buried in the center of the framework, it is connected to the transition metal-substituted on the periphery of the heteropolyanion through a bridging oxygen located trans to the open coordination site on the transition metal. The nature of this buried heteroatom should have little structural effect on chemical processes occurring on the periphery of the heteropolyanion so that the opportunity exists to observe effects on catalytic reactions arising from changes in formal potentials while keeping structural and environmental factors essentially constant. It was these features, as well as their anticipated resistance to conventional degradation processes, that attracted us to examine their electrochemical properties.

Some aspects of the electrochemistry of the parent heteropolyanions, $XW_{12}O_{40}^{m-}$, have been described in earlier studies (1,11). More recently, there has been extensive interest in the electrochemistry of these anions (12-14). They have been shown to be

useful for the modification of electrode surfaces (12,13) and have been incorporated in polymer films on electrodes (14). However, there has been little reported work on the electrochemical or electrocatalytic activity of the transition metal-substituted derivatives, even though they have potential to act as as inner-sphere as well as outer-sphere electron transfer catalysts. The only notable exception has been a report of the formal potentials of the $Mn^{II/III}$ couples of a series of the Mn substituted derivatives (7).

This thesis is mainly concerned with the electrochemical activity of the iron substituted ions (4). In chapter 2 their basic electrochemistry is presented. Formal potentials or a series of the ions are reported and pH and ionic strength effects are discussed. In chapter 3 the reactivity of the various oxidation states of the ions with H_2O_2, OH•, and O_2^- is presented. A high valent, formally Fe(IV) form of the ion was identified and its reactivity examined with a combination of electrochemical and pulse radiolysis techniques. A chain decomposition mechanism for H_2O_2 in which the iron center of the polyoxoanion shuttles between the +2, +3, and +4 oxidation states is proposed. In chapter 4 the electrocatalytic reduction of nitrous acid to ammonia, a net 6 electron process, is described. The ions are extremely selective in this reduction, and no hydroxylamine, a common intermediate when this process is catalyzed by other compounds, was formed. This unusual reactivity is attributed to the ability of the heteropolytungstates to deliver multiple electrons to the same substrate, which enables them to mimic the reactivity of biological enzymes. In chapter 5 the basic electrochemistry of some of the other

transition metal substituted heteropolytungstates is described.

Throughout this thesis the utility of the five anticipated advantageous characteristics of the transition metal substituted heteropolytungstates will be demonstrated. These compounds have been proven to be superior electrocatalysts, especially in terms of their durability, and hopefully work will continue in this area. The final chapter of this thesis contains a general overview of the electrochemical characteristics of several other transition substituted heteropolytungstates and would be a good starting point for further work.

REFERENCES

1. Pope, M. T., "Heteropoly and Isopoly Oxometallates" Springer-Verlag, Berlin, 1983, p. 59.

2. Baker, L.C.W.; Baker, V.E.S.; Eriks, K.; Pope, M.T.; Shibata, M.; Rollins, O.W.; Fang, J.H.; Koh, L.L., *J. Am. Chem. Soc.*, **1966**, *88*, 2329.

3. Ref. 1, p. 91.

4. (a) Zonnevijlle, F.; Tourne, C.M.; Tourne, F.T., *Inorg. Chem.*, **1983**, *22*, 1198. (b) ibid, **1982**, *21*, 2751.

5. Weakley, T.J.R., *J. Chem. Soc. Dalt. Trans.* **1973**, 341.

6. Weakley, T.J.R.; Malik, S.A., *J. Inorg. Nucl. Chem.*, **1967**, *29*, 2935.

7. Tourne, C.M.; Tourne, G.F.; Malik, S.A.; Weakley, T.J.R., *J. Inorg. Nucl. Chem.*, **1970**, *32*, 3875.

8. Katsoulis, D.E.; Pope, M.T.; *J. Am. Chem. Soc.*, **1984**, *106*, 2327.

9. Hill, C.L.; Brown, R.B., Jr., *J. Am. Chem. Soc.*, **1986**, *108*, 536.

10. Harmalker, S.H.; Pope, M.T., *J. Inorg. Biochem*, **1986**, *28*, 85.

11. Pope, M.T.; Varga, G.M., *Inorg. Chem.*, **1966**, *5*, 1249.

12. McEvoy, A.J.; Gratzel, J., *J. Electroanal Chem.*, **1986**, *209*, 391.

13. (a) Keita, B.; Nadjo, L., *J. Electroanal. Chem.*, **1988**, *240*, 325. (b) Keita, B.; Nadjo, L., *J. Electroanal. Chem.*, **1987**, *227*, 77. (c) Keita, B.; Nadjo, L.; Krier, G.; Muller, J.F., *J. Electroanal. Chem.*, **1987**, *223*, 287. (d) Keita, B.; Nadjo, L., *J. Electroanal. Chem.*, **1987**, *219*, 355.

14. (a) Keita, B.; Nadjo, L., *J. Electroanal. Chem.*, **1987**, *230*, 267. (b) Keita, B.; Nadjo, L., *J. Electroanal. Chem.*, **1986**, *208*, 343.

CHAPTER 2

ELECTROCHEMICAL PROPERTIES OF IRON(III) SUBSTITUTED HETEROPOLYTUNGSTATE ANIONS

ABSTRACT

The electrochemical behavior of a series of heteropolytungstate anions in which one of the W^{6+} cations is replaced by Fe^{3+} is described. The anions investigated were $FeXW_{11}O_{39}^{m-}$ (X = P, As, m = 4; X = Ge, Si, m = 5). All of the anions exhibit a reversible, one-electron couple associated with the Fe^{3+} center and a pair of two-electron waves attributed to electron addition and removal from the tungsten-oxo framework that comprises each anion's structure. The dependence of the formal potentials of the couples on pH and ionic strength is interpreted in terms of competition between protonation and ion-pairing of the reduced forms of the couples. The results are contrasted with the apparently less intricate behavior of the unsubstituted anions, $SiW_{12}O_{40}^{5-}$ and $PW_{12}O_{40}^{4-}$, which was recently described (8a).

ELECTROCHEMICAL PROPERTIES OF IRON(III) SUBSTITUTED HETEROPOLYTUNGSTATE ANIONS

INTRODUCTION

Traditional electrochemical catalysts are usually comprised of a transition metal center surrounded by one or more organic ligands. These organic ligands are susceptible to oxidative degradation by high energy intermediates formed during electron transfer processes. In the hope of discovering more robust catalysts we began the study of a series of transition metal substituted heteropolytungstates. These compounds are derived from the well-known Keggin structure ($SiW_{12}O_{39}^{-n}$) (1), by substituting a transition metal, in this case iron, for one of the twelve tungsten atoms (2,3). The tungsten oxo framework acts as a homoleptic pentadentate ligand with five bridging oxygen atoms available for coordination (2-5). The newly incorporated iron center provides a site where inner sphere electron transfer processes can occur (4). Thus it was believed that these molecules would show superior electrocatalytic activity compared to the unsubstituted ions that have been previously studied (6-9) yet retain their outstanding stability.

In this chapter the electrochemical behavior of a series of heteropolytungstates substituted with iron(III) is described. An interesting competition between ion pairing and protonation of the reduced ions is identified. The utility of such anions in catalytic applications, including the electrocatalytic reductions of H_2O_2, O_2

and HNO_2, will be described in the following chapters.

EXPERIMENTAL

Materials. The following salts of iron-substituted and lacunary heteropolytungstates were prepared as the α isomers and isolated by previously described procedures (4b): $K_8SiW_{11}O_{39}$, $K_5FeSiW_{11}O_{39}$, $K_8GeW_{11}O_{39}$, $K_5FeGeW_{11}O_{39}$, $K_7PW_{11}O_{39}$, $Rb_4FePW_{11}O_{39}$, $Rb_4FeAsW_{11}O_{39}$. $K_4SiW_{12}O_{40}$ was prepared according to the procedure of Baker and Pope (10). All salts were recrystallized twice from water, water-ethanol or water-methanol mixtures and dried in air. The water content of the isolated salts was estimated from thermogravimetric measurements based on the total loss in weight up to 200° C. Solutions of the reduced (Fe(II)) forms of the substituted anions were prepared by controlled potential electrolysis of solutions of the Fe(III) derivatives and were handled under argon using standard Schlenk line techniques. $NaClO_4$ was recrystallized twice from ethanol. Deionized water was further purified by passage through a purification train (Barnsted Nanopure). Prepurified argon was deoxygenated by passage through aqueous solutions of V(II). Other chemicals were reagent grade and were used as received. 0.1 M buffer solutions were prepared by partial neutralization of the following acids: HSO_4^- (pH 2); $Cl_2CHCOOH$ (pH 3); CH_3COOH (pH 3.5-6.0); morpholinoethanesulfonic acid, MES (pH 6-7); hydroxyethylpiperazinesulfonic acid, HEPES, (pH 7-8).

Apparatus and Procedures. Electrochemical measurements were conducted under argon in conventional two- or three-compartment cells with a glassy carbon working electrode, platinum wire counter electrode and a

sodium chloride saturated calomel reference electrode (SSCE). The working electrode (0.20 cm^2) was polished with 0.3 micron alumina and washed with purified water before use. Sonication of the polished electrode appeared to have no effect on the resulting responses. A combination of Princeton Applied Research instrumentation was used to record cyclic voltammograms and to conduct controlled potential electrolyses at stirred mercury pool electrodes. Thermogravimetric analyses were obtained with a Perkin-Elmer Model TGS 2 instrument equipped with a Model 3600 data-station.

Formal potentials were estimated as the average of the anodic and cathodic peak potentials at low scan rates (ca. 50 mV s^{-1}). Peak separations were typically 60-80 mV for the one-electron, iron-based waves and 40-60 mV for the two-electron tungsten-based waves. Experiments were conducted at ambient laboratory temperatures ($22\pm 2^{o}C$). All potentials are quoted with respect to the SSCE.

RESULTS AND DISCUSSION

Cyclic Voltammetry. Removal of one of the tungsten centers in a $XW_{12}O_{40}^{m-}$ anion and subsequent insertion of an Fe(III) center produced significant changes in the cyclic voltammetry exhibited by the anion. Voltammograms for the three silicon-based derivatives are displayed in Figure 2.1. The well-known set of three reversible waves that characterize the $SiW_{12}O_{40}^{4-}$ anion (6-9) is shown in Figure 2.1A. The set is comprised of two one-electron waves followed by a two-electron wave. These responses have all been assigned to the addition and removal of electrons from delocalized predominantly non-

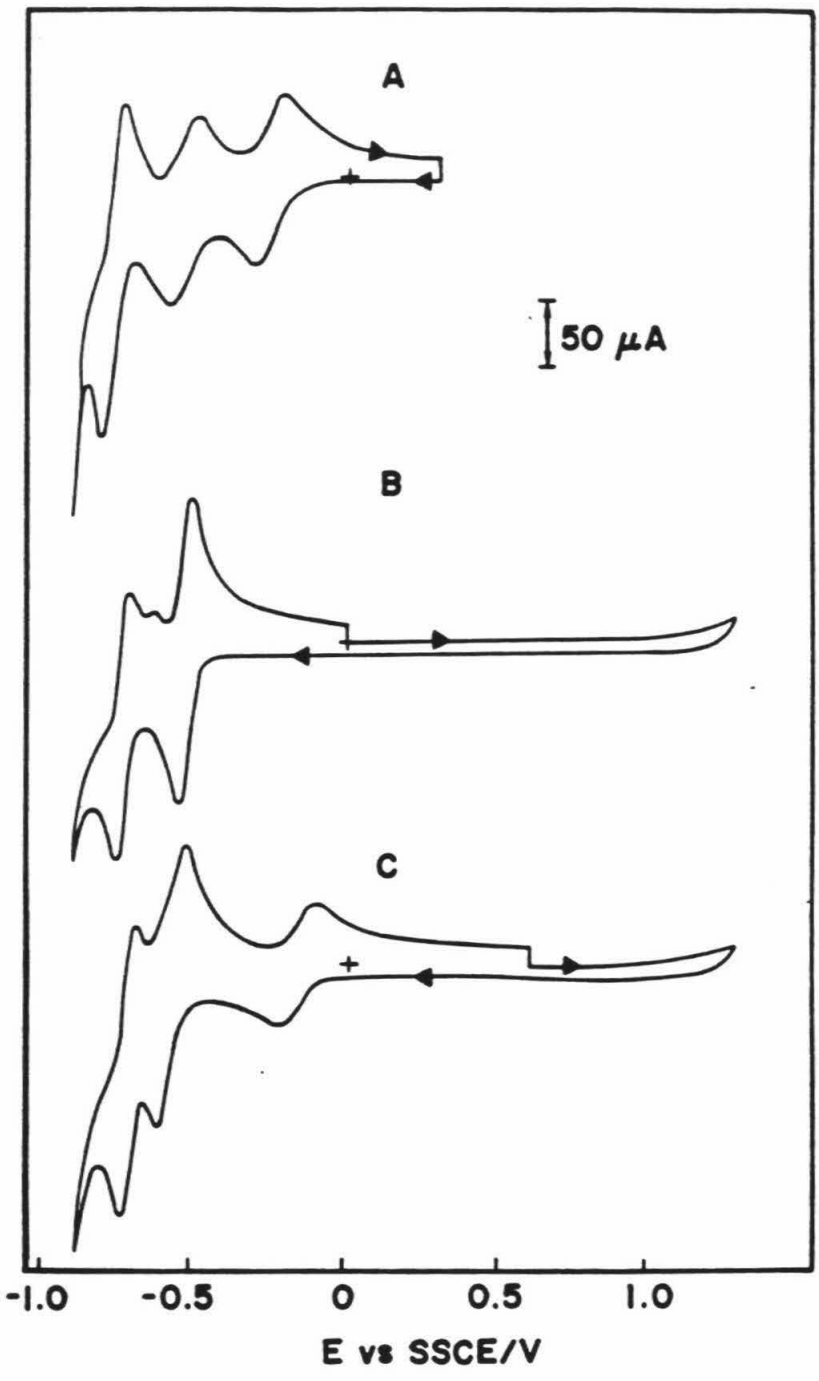

Figure 2.1. Cyclic voltammetry of 0.5 mM solutions of silicon-based heteropolytungstate anions at a glassy carbon electrode. (A) $SiW_{12}O_{40}^{4-}$;(B) $SiW_{11}O_{39}^{8-}$; (C) $FeSiW_{11}O_{39}^{5-}$. Supporting electrolyte: 0.1 M $NaClO_4$ + 0.01M $HClO_4$. Scan rate = 50 mV s-1.

bonding orbitals within the four tungsten-oxide triads within the polyanion (11,12). The response that results when a tungsten cation is removed from the polyanion is shown in Figure 2.1B and the voltammogram that results when the missing tungsten center is replaced with an iron(III) cation is shown in Figure 2.1C. The response for the lacunary $SiW_{11}O_{39}^{8-}$ anion contains two, two-electron waves with formal potentials significantly more negative than those for the first two waves of Figure 2.1A. (The behavior of $PW_{11}O_{39}^{7-}$ and $GeW_{11}O_{39}^{8-}$ is very similar.) The small anodic wave that appears between the two main waves in Figure 2.1B is believed to correspond to the β isomer of the anion which is known to be reduced at more positive potentials than the corresponding α isomer (13). The relative magnitude of the waves shows a scan rate dependence that is consistent with generation of the β isomer during reduction of the original α isomer at potentials on the second wave. Thus, at scan rates greater than 500 mV s^{-1} the anodic wave attributed to the a isomer is essentially absent while at scan rates below 5 mV s^{-1} this wave is as large as its cathodic counterpart and the anodic peak at the most negative potential is absent. The response in Figure 2.1C was obtained by adding a stoichiometric quantity of $Fe(NO_3)_3$ to the solution used to record Figure 2.1B. The positions of the two-electron waves for the lacunary anion are shifted slightly and a new reversible wave appears near -0.15 V. The absence of any response near 0.55 V indicates the absence of any free Fe^{3+} cations in solution and demonstrates the strong association of Fe^{3+} with the $SiW_{11}O_{39}^{8-}$ anion. An identical voltammogram was obtained with solutions prepared from the isolated

salt, $K_5FeSiW_{11}O_{39}\cdot H_2O$. Controlled potential reduction at -0.35 V showed that the new wave in Figure 2.1C involves one electron (1.05 electron per $H_2OFeSiW_{11}O_{39}^{5-}$ unit). The wave seems likely to correspond to the reduction of the coordinated Fe(III) center to Fe(II) as has been proposed in previous studies (4b).

Changes in the identity of the central heteroatom result in significant changes in the formal potential of the Fe^{III}/Fe^{II} wave in Figure 2.1C. The positions of the two-electron waves at more negative potentials are also influenced by changes in the heteroatom, but to a lesser extent. Formal potentials evaluated at pH 2.0 for the three sets of waves for four different heteroatoms are assembled in Table 2.1. Similar shifts have been reported for the $Mn^{III}/^{II}$ couples in the Mn substituted derivatives (5). A correlation has also been previously noted between the formal potentials and the formal charges of unsubstituted $XW_{12}O_{40}^{m-}$ anions (6). The data in Table 1.1 make it clear that there is no such simple correlation for the $FeXW_{11}O_{39}^{n-}$ series.

Effect of pH. $FeSiW_{11}O_{39}^{5-}$, $FeGeW_{11}O_{39}^{5-}$, and $FePW_{11}O_{39}^{4-}$ are stable in aqueous media between pH 2 and 8 and $FeAsW_{11}O_{39}^{4-}$ is stable between pH 2 and 6. Outside of this pH range the iron-substituted heteropolyanions are unstable with respect to hydrolytic decomposition. Within their stable pH ranges the formal potentials for all three sets of waves in Figure 2.1 are dependent on pH, although to differing extents. In Figure 2.2 the formal potentials for the two, two-electron waves for the $SiW_{11}O_{39}^{5-}$ anion are plotted versus pH in the range where the polyanion is stable. The redox

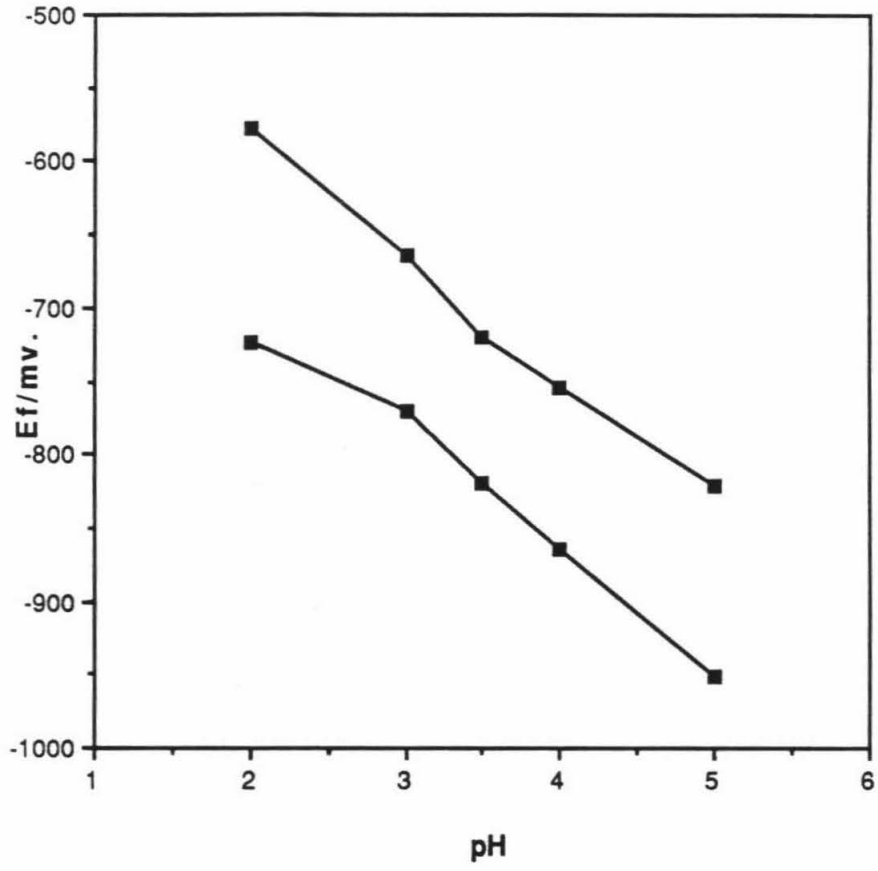

Figure 2.2. pH dependence of formal potentials for the two-electron redox couples exhibited by $FeSiW_{11}O_{39}^{5-}$. (A) First two-electron wave; (B)Second two-electron wave. The iron-substituted heteropolytungstates based on Ge, P and As behaved similarly. Supporting electrolyte: 0.1 M Na^+ plus buffers listed in the Experimental Section.

process involved is usually assigned to reduction and re-oxidation of the tungsten-oxide framework of the anion and the behavior of the silicon-heteropolytungstate is representative of that of all four anions examined. The slopes of the plots are not pH dependent and lie in the range of 60 to 90 mV per pH unit, indicative of the addition of two to three protons to the reduced forms of each redox couple. The behavior is very similar to that exhibited by the two-electron wave of the unsubstituted $SiW_{12}O_{40}^{5-}$ anion that has been interpreted on the same basis (6). Recent Evans determination experiments have shown the doubly reduced parent ion $PW_{12}O_{40}^{-5}$ is more diamagnetic than the unreduced ion. This result has been interpreted as indicating that the electrons go into extremely delocalized orbitals encompassing the entire tungsten oxide framework, which results in ring currents similar to those found in benzene(12). A summary of the formal potentials measured at pH 2 is given in Table 2.1. At pH values above 5 the separation between the cathodic and anodic peak potentials of the waves becomes larger (> 150 mV) and it is difficult to obtain reliable estimates of the formal potentials.

The pH dependence of the formal potentials of the one-electron $Fe^{III/II}$ waves is more intricate than that of the two-electron waves, as shown in Figure 2.3. The pH dependences exhibited by the $H_2OFeSiW_{11}O_{39}^{5-}$ and $H_2OFeGeW_{11}O_{39}^{5-}$anions at high and low pH values is separated by a region of virtual pH independence between pH 3.5 and 6.5. The less highly charged $H_2OFePW_{11}O_{39}^{4-}$ and $H_2OFeAsW_{11}O_{39}^{4-}$ anions behave similarly except that the range of pH independence is somewhat narrower.

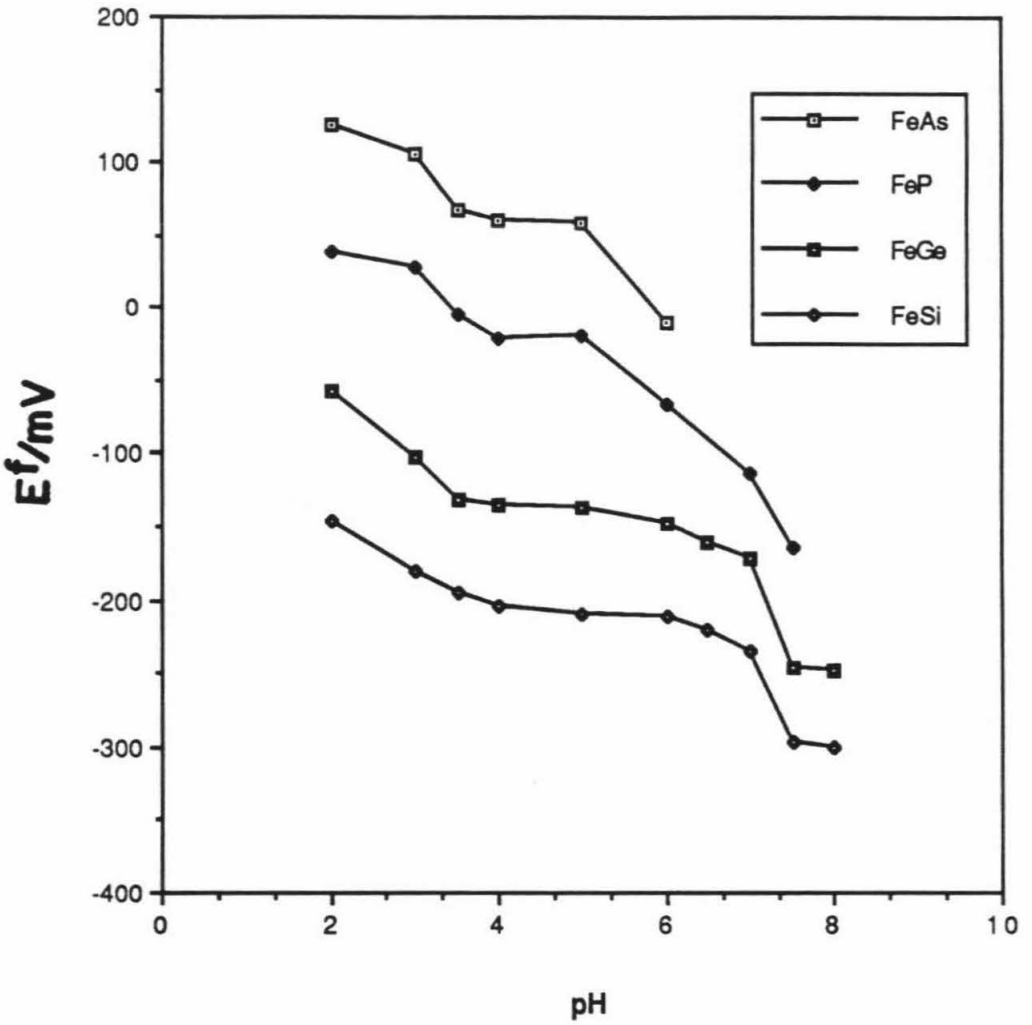

Figure 2.3. pH dependence of formal potentials for the first, one-electron redox couple exhibited by four, iron-substituted heteropolytungstates, $FeXW_{11}O_{39}^{n-}$. The heteroatom, X, is indicated in the Figure. Supporting electrolytes as in Figure 2.2.

The behavior shown in Figure 2.3 is not consistent with the pKa value of 5.2 that has been reported for the single water molecule coordinated to the Fe(III) center in $H_2OFeSiW_{11}O_{39}^{5-}$ (4b). Because of this discrepancy, acid-base titrations of solutions of $K_5FeSiW_{11}O_{39}$ and mixtures of the anion with $HClO_4$ were performed. The titration curve for the anion alone, shown in the upper curve in Figure 2.4, matches that expected for a monoprotic weak acid with a pKa of 6.3. The titration curve obtained for a mixture of $HClO_4$ and $K_5FeSiW_{11}O_{39}$ (lower curve in Figure 2.4) demonstrates the absence of any weakly acidic groups with pKa values below pH 4.5. Thus, it can be concluded that neither the bridging nor the terminal oxide ions of the $H_2OFeSiW_{11}O_{39}^{5-}$ anion are protonated at pH values as low as 2. It was not possible to examine the behavior in more acidic solutions because of the decomposition of the heteropolyanion.

The pKa value of 6.3 for the $H_2OFeSiW_{11}O_{39}^{5-}$ anion obtained from the pH titration is in moderately good agreement with the value that can be estimated from the intersection of the dashed lines drawn through the data points in Figure 2.3 (pKa = ca. 6.8). It therefore seems likely that the previously reported pKa for $H_2OFeSiW_{11}O_{39}^{5-}$ (4b) is approximately one unit too low. The data in Figure 2.3 lead to a pKa of 5.3 for the $H_2OFePW_{11}O_{39}^{4-}$ anion, which is also about one unit higher than the previously reported value (4b).

The dimerization of $HOFeSiW_{11}O_{39}^{6-}$ has been reported to proceed with an equilibrium constant of ca. 40 m^{-1} (4b). With such a small value of the equilibrium constant, dimerization would not complicate pH titrations of millimolar solutions of the heteropolyanion and no

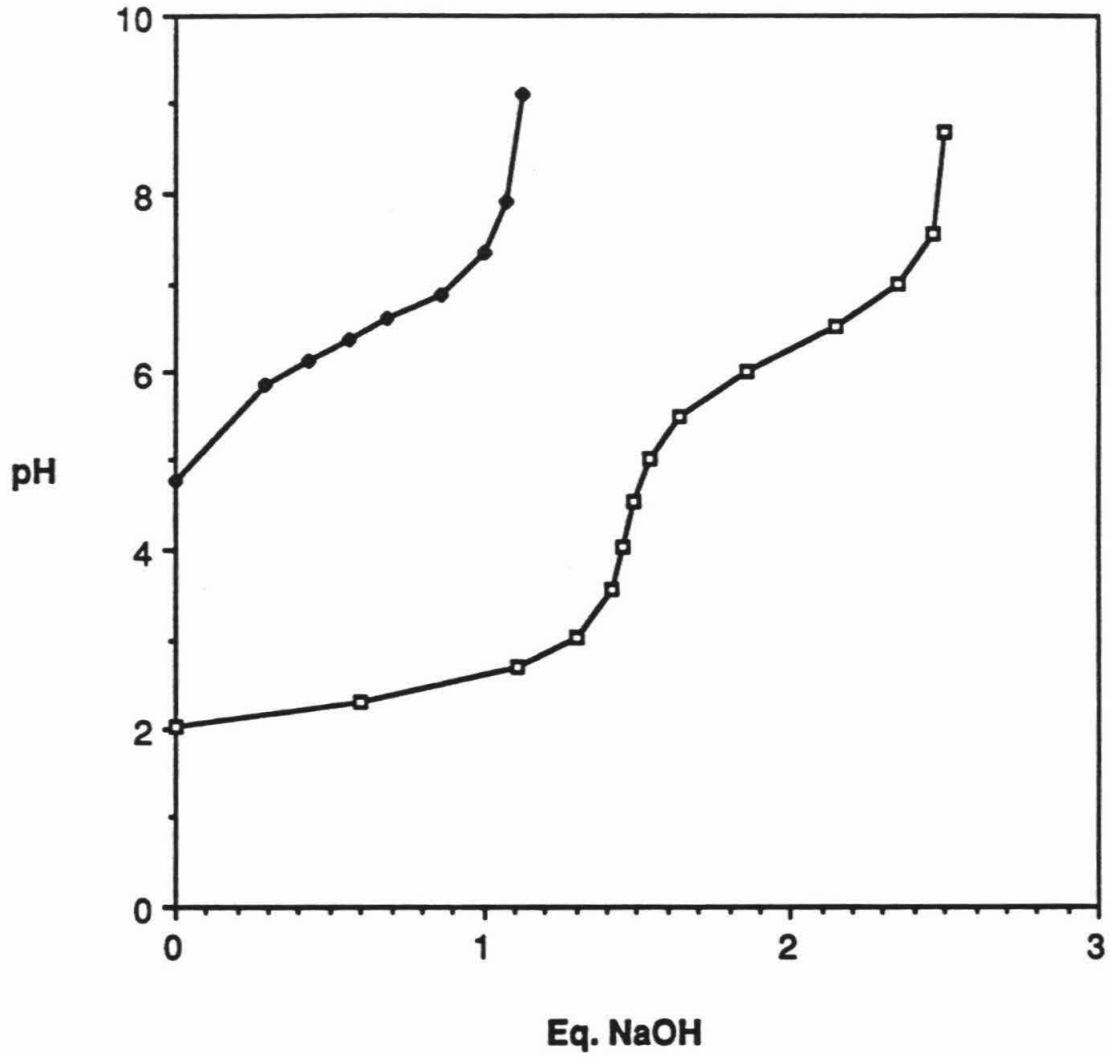

Figure 2.4. Titration of $H_2OFeSiW_{11}O_{39}^{5-}$ with NaOH. (A) 1 mM $H_2OFeSiW_{11}O_{39}^{5-}$ in H_2O. (B) 6.67 mM $H_2OFeSiW_{11}O_{39}^{5-}$ in 0.1 M $NaClO_4$ + 0.01 M $HClO_4$. The abscissa is the moles of NaOH added per mole of $H_2OFeSiW_{11}O_{39}^{5-}$ present.

evidence for dimer formation was encountered. However, spectral data presented in reference 4b are not compatible with the quoted dimerization constant and no detailed description was provided of the experimental measurements from which the constant was estimated. Thus, the quantitative aspects of the possible dimerization of $HOFeSiW_{11}O_{39}^{6-}$ anions remain to be determined.

The increases in the Ef values in Figure 2.3 at pH values below 3 could reflect protonation of a bridging oxide ion in the reduced form of the anions at low pH.

Effect of Ionic Strength. The average negative charge density on unsubstituted parent anions such as $SiW_{12}O_{40}^{4-}$ and $PW_{12}O_{40}^{3-}$ is smaller than that of ions such as SO_4^{2-} or $Fe(CN)_6^{4-}$ that are known to form ion-pairs with alkalia cations. However, the iron-substituted derivatives bear greater negative charges, which would favor the formation of ion-pairs with cations of the supporting electrolyte. One result of this could be changes in the measured formal potentials. This possibility was examined by measuring formal potentials for the first, iron-centered wave of the representative $H_2OFeGeW_{11}O_{39}^{5-}$ anion in a variety of supporting electrolytes. The results are summarized in Table 2.2. At a constant pH of 5.0, increasing the concentration of the $NaClO_4$ supporting electrolyte produces significant positive shifts in the formal potential. Identical shifts in potential are observed with chloride salts so that the identity of the supporting electrolyte anion seems unimportant. If both the pH and the ionic strength are kept constant while the identity of the supporting electrolyte cation is changed, positive shifts in formal potentials

are observed with the magnitude of the shift increasing in the order $Rb^+ > K^+ > Na^+ > Li^+$ (Table 2.2A). Both trends are in the order expected for stronger ion-pairing between the supporting electrolyte cation and the more highly charged, reduced form of the heteropolyanion.

In a recent electrochemical study of the unsubstituted parent anion, $SiW_{12}O_{40}^{4-}$, which was restricted to acidic solutions, a similar ionic strength effect was reported for the first, one-electron wave (9). It was concluded that the observed shifts in formal potentials were the result of large changes in liquid junction potentials. This alternative interpretation is not supported by the data in Table 2.2A for the iron-substituted ions at these higher pH values. For example, the ratio of the ionic mobilities of Na^+ and K^+ is larger than the ratio for K^+ and Rb^+, so that liquid junction calculations would predict a larger shift in apparent Ef values when Na^+ was substituted by K^+ than when K^+ was substituted by Rb^+. Experimentally the opposite is found (Table 2.2A), *i.e.*, the shift in apparent formal potential is greater for the latter pair of supporting electrolytes. It would be of interest to extend the studies of the parent $XW_{12}O_{40}^{m-}$ ions to higher pH values to see if the behavior of the unsubstituted and substituted heteropolyanions is less disparate in less acidic media. In any case, the proposal that the first redox couple of unsubstituted anions such as $SiW_{12}O_{40}^{4-}$ could be attractive as redox probes with formal potentials independent of the pH or ionic strength of the media (9) is clearly not appropriate for the iron-substituted derivatives.

It is instructive to compare the shifts in the formal potentials produced by increases in the concentration of the $NaClO_4$ supporting electrolyte at several pH values. The necessary data are listed in Table 2.2B for the $H_20FeGeW_{11}O_{39}^{5-}$ anion. Changes in ionic strength produce the largest effects on Ef values in the pH ranges where Ef is least dependent on pH (figure 2.5). Thus, the largest shift in Ef produced from increasing the concentration of $NaClO_4$ from 0.1 M to 1.1 M occurs at pH 5, where the plot of E_f for the $H_20FeGeW_{11}O_{39}^{5-}$ anion vs pH in Figure 2.5 has almost no slope. At the lower and higher pH values where E_f becomes more pH-dependent, its dependence on ionic strength diminishes. The behavior can be understood as resulting from a competition between protonation and ion-pairing in order to decrease the net negative charge of the reduced form of the heteropolyanion: At low pH, protonation is more pronounced while at higher pH, sodium ion-pairing supplants protonation. The pH independent regions of the curves in Figure 2.5 represent the range where sodium ion-pairing has replaced proton binding completely. At still higher pH values (*e.g.*, above 6.5 for $H_2OFeSiW_{11}O_{39}^{5-}$) the aquo ligand bound to the iron(III) center is converted to a hydroxo ligand that is presumably protonated in the reduced (Fe(II)) form of the anion so that the dependence on ionic strength is again diminished. This interdependence of ionic strength and pH effects is further evidence that at least the reduced, Fe(II) forms of the ions are somewhat ion paired in solution.

The two-electron waves that are present at more negative potentials also exhibit dependences on pH and ionic strength that are consistent

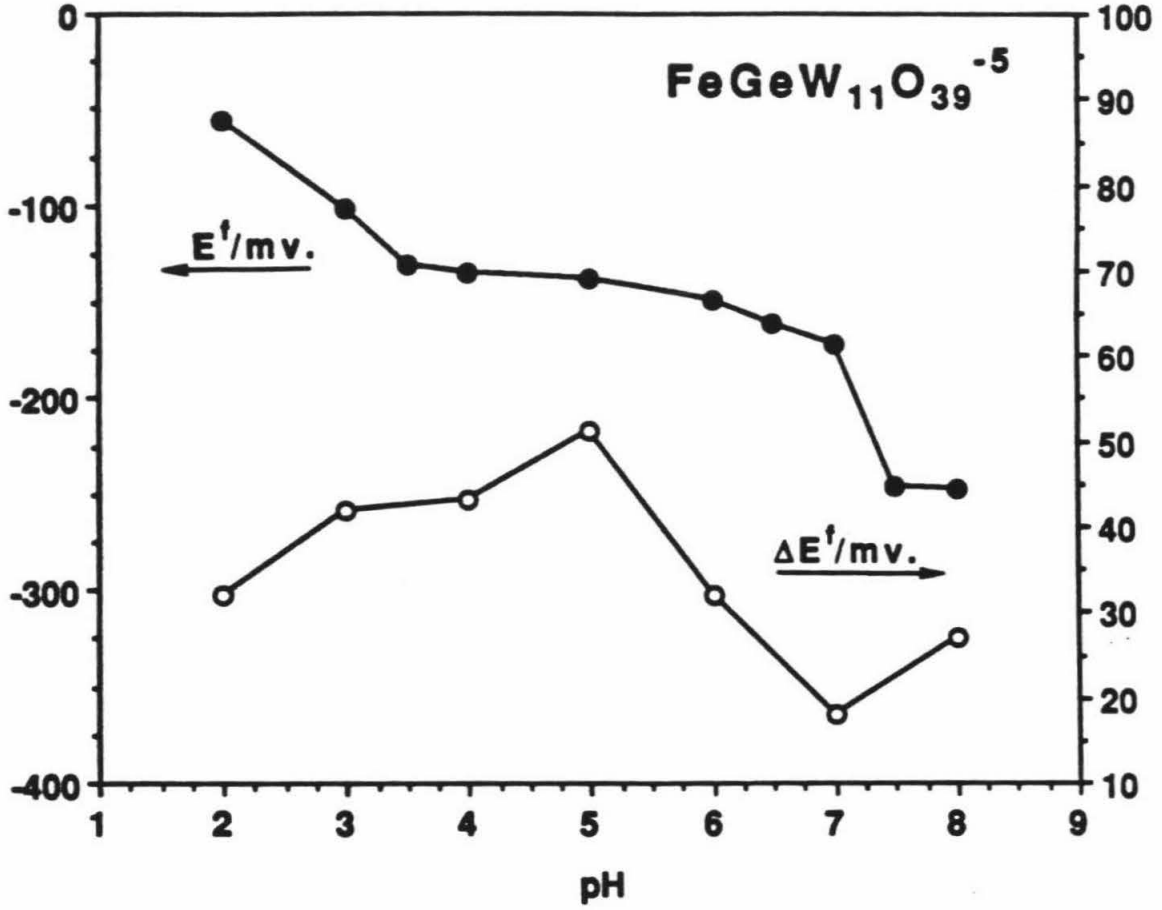

Figure 2.5. Comparison of pH and ionic strength effects on E^f of $Fe^{II/III}$ couple of $H_2OFeGeW_{11}O_{39}^{5-}$.(A) E^f (left axis) at a given pH, buffers as listed in experimental. (B) Change in E^f (right axis) on changing ionic strength from 0.1 M to 1.0 M at a given pH.

with competition between protonation and ion-pairing. For example, at pH 2 the formal potentials for both two-electron waves of $H_2OFe^{II}GeW_{11}O_{39}(^{6-}$ increase by only 14 mV when the sodium ion concentration is increased from 0.1 to 1.1 M. However, at pH 6 the same change in supporting electrolyte concentration produces an increase in E_f of ca. 60 mV.

CONCLUSIONS

The electrochemistry of a series of Fe(III)-substituted heteropolyanions of the class $H_2OFeXW_{11}O_{39}^{n-}$(X = Si, Ge, P, As) differs significantly from that of the unsubstituted parent heteropolyanion $XW_{12}O_{40}^{m-}$. The substituted anions exhibit one, one-electron wave appearing to be associated with reduction of the iron center and two two-electron waves associated with reduction of the tungsten-oxo framework. The formal potentials of the reversible $Fe^{III/II}$ couples are dependent on both pH and ionic strength because of competition between protonation and ion-pairing reactions with the reduced forms of the ions. The reductions of the tungsten oxo centers appear to be accompanied by multiple protonations.

REFERENCES

1. Pope, M. T., "Heteropoly and Isopoly Oxometallates" Springer-Verlag, Berlin, 1983, p. 59.

2. Baker, L.C.W.; Baker, V.E.S.; Eriks, K.; Pope, M.T.; Shibata, M.; Rollins, O.W.; Fang, J.H.; Koh, L.L., *J. Am. Chem. Soc.*, **1966**, *88*, 2329.

3. Ref. 1, p. 91.

4. (a) Zonnevijlle, F.; Tourne, C.M.; Tourne, F.T., *Inorg. Chem.*, **1983**, *22*, 1198. (b) ibid, **1982**, *21*, 2751.

5. Tourne, C.M.; Tourne, G.F.; Malik, S.A.; Weakley, T.J.R., *J. Inorg. Nucl. Chem.*, **1970**, *32*, 3875.

6. Pope, M.T.; Varga, G.M., *Inorg. Chem.*, **1966**, *5*, 1249.

7. McEvoy, A.J.; Gratzel, J., *J. Electroanal Chem.*, **1986**, *209*, 391.

8. (a) Keita, B.; Nadjo, L., *J. Electroanal. Chem.*, **1988**, *240*, 325. (b) Keita, B.; Nadjo, L., *J. Electroanal. Chem.*, **1987**, *227*, 77. (c) Keita, B.; Nadjo, L.; Krier, G.; Muller, J.F., *J. Electroanal. Chem.*, **1987**, *223*, 287. (d) Keita, B.; Nadjo, L., *J. Electroanal. Chem.*, **1987**, *219*, 355.

9. (a) Keita, B.; Nadjo, L., *J. Electroanal. Chem.*, **1987**, *230*, 267. (b) Keita, B.; Nadjo, L., *J. Electroanal. Chem.*, **1986**, *208*, 343.

10. Baker, L.C.W.; Pope, M.T., *J. Am. Chem. Soc.*1960, *82*, 4176.

11. Ref. 1, p. 101.

12. Kozik, M.; Casan-Pastor, N.; Hammer, C.F.; Baker, L.C.W., *J. Am. Chem. Soc.*, **1988**, *110*, 7597.

13. Ref. 1, p. 105.

TABLE 2.1

Formal potentials of the three redox couples exhibited by $FeXW_{11}O_{39}^{Z-}$ heteropolyanions. [a,b]

X	Z	One-electron wave (Fe(III)/Fe(II))	Z	First two-electron wave	Z	Second two-electron wave
Si(V)	-5	-0.145	-6	-0.580	-8	-0.720
Ge(IV)	-5	-0.065	-6	-0.557	-8	-0.666
P(V)	-4	0.039	-5	-0.560	-7	-0.706
As(V)	-4	0.123	-5	-0.537	-7	-0.655

a. Entries are in volts vs. SSCE.

b. Supporting electrolyte: 0.1 M $NaClO_4$ + 0.01 M $HClO_4$. T = 22 ± 2° C.

TABLE 2.2

Formal Potentials of the Fe^{III}/Fe^{II} couple of $H_2OFeGeW_{11}O_{39}^{5-}$ in various supporting electrolytes

A. Fixed pH (5)

Counter-ion	Counter-ion conc., M	E^f, mV	ΔE^f, mV
Na +	0.001	-171	-34
Na +	0.1	-137	0
Na +	1.1	-86	+ 51
Li +	1.1	-95	+ 42
K +	1.1	-77	+ 60
Rb +	1.1	-62	+ 75

B. Fixed counter-ion (Na +)

pH	E^f, mV $[Na^+] = 0.1$ M	E^f, mV $[Na^+] = 1.1$ M	ΔE^f, mV
2.0	-50	-18	+ 32
3.0	-102	-60	+ 42
4.0	-135	-92	+ 43
5.0	-137	-86	+ 51
6.0	-149	-117	+ 32
7.0	-172	-190	+ 18
8.0	-247	-220	+ 27

CHAPTER 3

ELECTROCHEMISTRY AND REDOX CHEMISTRY OF $H_2OFe^{III}SiW_{11}O_{39}^{5-}$ IN THE PRESENCE OF H_2O_2 AND OH

ABSTRACT

Heteropolytungstates in which one of the positions normally occupied by a tungsten cation is occupied instead by an iron cation are shown to be electrocatalysts for the electroreduction of H_2O_2. The rate constant governing the reduction of H_2O_2 by $H_2OFe^{II}SiW_{11}O_{39}^{6-}$ was measured by stopped flow as 9×10^2 M^{-1} s^{-1}. A catalytic mechanism involving a Fe(IV) intermediate generated from the reaction between the Fe(III) form of the heteropolytungstate anion and hydroxyl radicals is proposed. The Fe(IV) intermediate can react with itself to produce H_2O_2 and the Fe(III) form of the heteropolytungstate. Alternatively the Fe(IV) intermediate can consume additional H_2O_2 by oxidizing it to O_2. Competition between these two reaction pathways accounts for the non-integral stoichiometry observed under some experimental conditions during the electroreduction of H_2O_2 catalyzed by $H_2OFe^{II}SiW_{11}O_{39}^{6-}$. Pulse radiolysis experiments were employed to detect the Fe(IV) intermediate, to evaluate rate constants for the reactions in which it is formed and decomposed, and for the reduction of the Fe(III) form of the heteropolytungstate by $O_2^{\cdot-}$.

ELECTROCHEMISTRY AND REDOX CHEMISTRY OF $H_2OFe^{III}SiW_{11}O_{39}^{5-}$ IN THE PRESENCE OF H_2O_2 AND OH

INTRODUCTION

With the goal of identifying electrocatalytically active transition metal complexes that are more resistant to oxidizing environments than are those based on organic ligands, we have been examining the electrochemistry of transition metal-substituted heteropolytungstates (1,2). The initial studies, which were described in the previous chapter of this thesis, involved a series of iron-substituted anions, $H_2OFe^{III}XW_{11}O_{39}^{n-}$, where X represents a tetrahedrally coordinated heteroatom (Si, Ge, P, As) surrounded by four triads of tungsten-oxo octahedra (3). The resulting, polynuclear structure retains its integrity in aqueous media over a broad pH range ($2 < pH < 8$) and the entirely inorganic complexes are inert toward oxidizing agents that often degrade complexes containing organic ligands. In the $H_2OFe^{III}XW_{11}O_{39}^{n-}$ complexes, the tungsten-oxo framework provides a vacant coordination site composed of five bridging oxo groups in which the Fe(III) center sits. The sixth coordination position of the Fe(III) cation is occupied by a substitutionally labile water molecule (which is converted to a hydroxide ion at higher pH values, *e.g.*, pH 6 for X = Si (1,3)). Suitable substrates can displace the labile water molecules on the iron center so that electron transfer between the heteropoly-anion and reducible or oxidizable substrates can proceed by inner-sphere mechanisms that are not available to the more commonly

studied, unsubstituted anions such as $SiW_{12}O_{40}^{4-}$ (4).

In chapter 4 the catalytic utility and robustness of the $H_2OFe^{III}SiW_{11}O_{39}^{5-}$ anion will be demonstrated in a study of the electrocatalytic reduction of nitrite and nitric oxide (2). The anion is also catalytically active toward the electro-reduction of H_2O_2 where highly oxidizing hydroxyl radicals are likely intermediates. We undertook a study of this system to expand the range of substrates for which kinetic data on the catalytic efficiency of this class of catalyst were available as well as to assess their resistance to oxidative degradation by hydroxyl radicals. The electrochemical experiments revealed reactions of the catalyst that differed substantially from those proposed for other electrocatalysts for the electroreduction of H_2O_2 such as $Fe(OH_2)_6^{3+}$ (5). A short-lived form of the catalyst with the iron center oxidized to an oxidation state above +3 was implicated. Pulse radiolysis experiments were successful in detecting the indicated intermediate and allowed its rate of formation and disappearance as well as some of its redox reactions to be monitored. This chapter summarizes the result of the electrochemical and pulse radiolysis experiments and utilizes the results of the latter to rationalize the unusual behavior observed in the former set of experiments.

EXPERIMENTAL

Materials. The heteropolytungstate anions were prepared and purified as previously described (1,3). Other chemicals for electrochemical experiments were reagent grade and used as received. Stock solutions

of H_2O_2 were analyzed regularly by titration with standard solutions of $KMnO_4$ (6).

Electrochemical Apparatus and Procedures. The electrochemical instrumentation and procedures employed have been described (1). Polished, glassy carbon electrodes (Tokai Co., Tokyo) were utilized for cyclic voltammetry and rotating disk voltammetry. Controlled potential electrolyses were conducted at a stirred mercury pool electrode. Potentials were measured and are reported with respect to a sodium chloride saturated calomel electrode (SSCE) except where noted. Experiments were conducted under Argon at ambient laboratory temperatures (20-23^{o} C).

Radiolysis Apparatus and Procedures. All solutions for radiolysis experiments were prepared with water which, after distillation, was passed through a Milli-Q purification system.

The pulse radiolysis experiments were carried out with solutions containing 0.1 M sodium perchlorate and 2-50 mM. phosphate. Their pH was adjusted by addition of small amounts of $HClO_4$ or NaOH. The chemicals and gases ($NaClO_4 \cdot H_2O$, G.F. Smith Chem. Co.; HCOONa, 'Baker Analyzed' reagent; NaOH, G.F. Smith Co Ultrapure 99.999%; H_2SO_4, J.T. Baker Chemical Co., Ultrex; KH_2PO_4, J.T. Baker Chemical Co., Ultrex; N_2O and O_2 both UHP grade from MG Gases Ltd.) were used as received.

Upon radiolysis of water with ionizing radiation (^{60}Co - γ rays or 2 MeV electrons) the following radicals and molecular products are formed:

$$H_2O \rightsquigarrow HO\bullet(2.75),\ e^-_{aq}(2.65),\ H\bullet(0.55),\ H_2O_2(0.72),\ H_2(0.45) \qquad (1)$$

where the values in parenthesis are G values, that is, the number of species formed when 100 eV of energy is dissipated in water(7). Saturation of an aqueous solution with N_2O at pH > 4 results in the effective conversion of all e^-_{aq} to OH radicals by the well-established mechanism ($k(e^-_{aq} + N_2O + H_2O \rightarrow N_2 + HO\bullet + HO^-) = 8.7 \times 10^9\ M^{-1}\ s^{-1}$ (8)). Added formate reacts rapidly with both HO and H yielding the CO_2^- radical ($k(HO + HCOO^- \rightarrow H_2O + CO_2^-) = 3.2 \times 10^9\ M^{-1}\ s^{-1}$) and ($k(H + HCOO^- \rightarrow H_2 + CO_2^-) = 2.1 \times 10^8\ M^{-1}\ s^{-1}$)(9). The hydrated electron reacts with the proton at a diffusion controlled rate yielding H atoms ($k\ (e^-_{aq} + H^+ \rightarrow H) = 2.3 \times 10^{10}\ M^{-1}\ s^{-1}$; pK ($H \rightleftharpoons H^+ + e^-_{aq}$) = 9.6)(9). The O_2^-/HO_2 radicals (pK = 4.8) are formed either by direct oxygen scavenging of the primary reducing radicals ($k(e^-_{aq}/H + O_2 \rightarrow O_2^-/HO_2) = 2.0 \times 10^{10}\ M^{-1}\ s^{-1}$) or via the CO_2^- radical reaction with O_2 ($k(CO_2^- + O_2 \rightarrow CO_2 + O_2^-) = 5.0 \times 10^9\ M^{-1}\ s^{-1}$)(10).

Pulse radiolysis experiments were carried out with the BNL 2 MeV Van de Graaff Accelerator according to procedures described elsewhere(11). Calibration of the energy deposition was done with the KSCN dosimeter taking $G((SCN^-)^{2-}) = 6.13$ and $\varepsilon_{472} = 7950\ M^{-1}\ cm^{-1}$.

Steady state radiolyses were performed in a ^{60}Co gamma-ray source which had been calibrated with the ferrous dosimeter using $G(Fe^{3+}) = 15.5$(12); the energy flux at the time was 1.0 krad/min or 1.0×10^{-7} M of OH radicals per second. All peroxide concentrations of radiolyzed solutions were determined with the KI method(13).

Stopped flow experiments were performed under nitrogen with a Durrum Instrument Model # D-110 stopped flow spectrophotometer, which

was interfaced to an "Olis" data evaluation system.

RESULTS

Electrochemistry of $H_2OFeSiW_{11}O_{39}^{5-}$ in the presence of H_2O_2. The electrochemical responses exhibited by the $H_2OFe^{III}SiW_{11}O_{39}^{5-}$ anion in the absence of reducible substrates have been described in a previous study (1). The dashed curve in Figure 3.1A is a representative cyclic voltammogram that consists of three reversible couples. The response at the most positive potential involves the one-electron Fe^{III}/Fe^{II} couple and the two waves at more negative potentials arise from separated, two-electron reductions of the tungsten-oxo framework. Addition of H_2O_2 to the solution of $H_2OFe^{III}SiW_{11}O_{39}^{5-}$ produced a large increase in the cathodic peak current at the potential where the Fe(III) center is reduced to Fe(II) (Figure 3.1A, solid line) and the catalyzed reduction of H_2O_2 ensued. It is clear that the Fe center plays an essential role in the catalytic mechanism because the cyclic voltammetry of the unsubstituted $SiW_{12}O_{40}^{4-}$ anion, which has a one-electron reduction wave at almost the same potential as the $Fe^{III}SiW_{11}O_{39}^{5-}$ derivative, showed no evidence of a catalytic reduction when H_2O_2 was added (Figure 3.1B). (The reduced, iron-free anion, $SiW_{12}O_{40}^{5-}$, does react slowly with H_2O_2 but the reaction rate is too low to affect cyclic voltammetric responses at scan rates of 100 mV s^{-1}. In a preliminary study, the kinetics of the reaction were zero order in reduced tungstate and zero order in H_2O_2. The reaction was first order in the initial amount of tungstate, whether oxidized or reduced. One possible explanation of these curious results is that

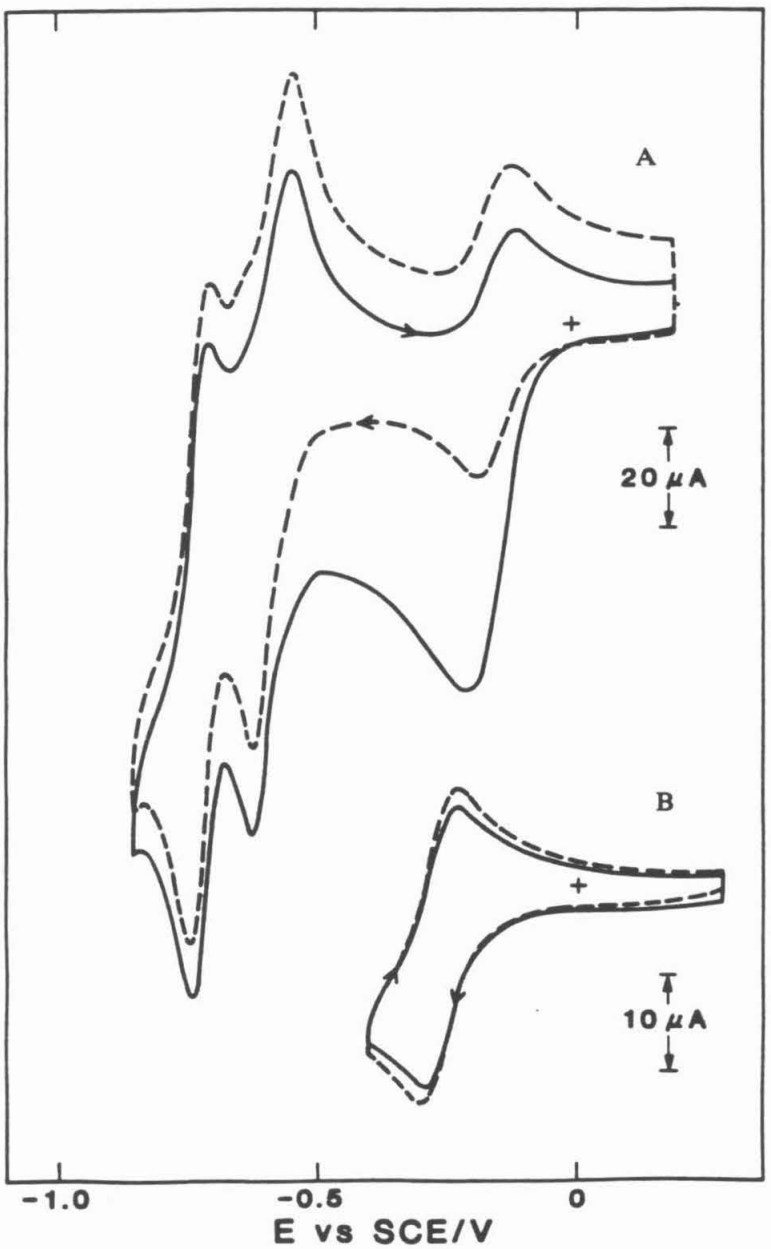

Figure 3.1. Cyclic voltammograms of 1 mM solutions of $H_2OFe^{III}SiW_{11}O_{39}^{5-}$ (A) and $SiW_{12}O_{40}^{4-}$ (B) before (- - - -) and after (——) addition of 1 mM H_2O_2. Scan rate = 50 mV s^{-1}. Supporting electrolyte: 0.1 M $NaClO_4$ + 0.01 M $HClO_4$.

the $SiW_{12}O_{40}^{4-}$ structure, whether oxidized or reduced, breaks up to expose open tungsten coordination sites at which the H_2O_2 can bind prior to reduction. (These preliminary results were not pursued in any detail.)

Controlled potential electrolyses of mixtures of $H_2OFe^{III}SiW_{11}O_{39}^{5-}$ and H_2O_2 at -0.4 V, where the Fe(III) center in the catalyst is reduced to Fe(II), proceeded smoothly and consumed between 0.9 and 2 electrons per H_2O_2 molecule, depending on the relative concentrations of the catalyst and H_2O_2 and the solution pH. The catalyst was unaffected by extensive cycling during electrolytic reductions as judged by its cyclic voltammetry before and after the electrolysis. The variable quantity of charge consumed during the electrolysis contrasts with the behavior observed when $Fe(OH_2)_6^{3+}$ is employed as catalyst for the electroreduction of H_2O_2 (5): Two electrons are consumed by each H_2O_2 molecule according to a proposed reaction sequence in which hydroxyl radicals produced in the first step are quantitatively reduced by Fe(II) in a rapid second step (5). When the electroreduction was carried out with the $H_2OFe^{III}SiW_{11}O_{39}^{5-}$ catalyst at more negative potentials, where the two-electron reduction of the tungsten oxo framework proceeds along with the reduction of the Fe(III) center to produce a species capable of transferring more than one electron, two electrons per H_2O_2 molecule were required. The consumption of fewer than two electrons per H_2O_2 molecule during the catalyzed electroreduction of H_2O_2 at potentials where only the Fe(III) center of the $H_2OFe^{III}SiW_{11}O_{39}^{5-}$ anion is reduced suggests the existence of a reaction pathway involving the

iron center in which the hydroxyl radicals generated in the primary reaction between H_2O_2 and $H_2OFe^{II}SiW_{11}O_{39}^{6-}$ are diverted into a reaction other than further reduction by a second $H_2OFe^{II}SiW_{11}O_{39}^{6-}$ anion. Further consideration of this alternative reaction pathway will be deferred to the Discussion section.

In a separate set of experiments, the rate of reaction between H_2O_2 and $H_2OFe^{II}SiW_{11}O_{39}^{6-}$ was measured using stopped-flow techniques. The reaction was examined with large excesses of the reduced anion present which avoided the complications of non-integral stoichiometry encountered in the electrochemical measurements. Clean second-order kinetics were observed ($k = 9 \pm 0.3) \times 10^2$ M^{-1} s^{-1}) which were consistent with a slow initial step producing a hydroxyl radical that was subsequently rapidly reduced by a second $H_2OFe^{II}SiW_{11}O_{39}^{6-}$ anion.

It also proved instructive to carry out electroreductions of H_2O_2 as catalyzed by $Fe(OH_2)_6^{3+}$ in the presence of the $H_2OFe^{III}SiW_{11}O_{39}^{5-}$ or $SiW_{12}O_{40}^{4-}$ anions. In the absence of the heteropolytungstates the electroreductions of the H_2O_2 followed a simple two-electron pathway as described in previous reports (5). In the absence of H_2O_2, addition of either heteropolytungstate was without effect on the voltammetric response of the $Fe(OH_2)_6^{3+/2+}$ couple that occurs at a much more positive potential (E^o = 0.50 V) than the first reduction wave of $H_2OFeSiW_{11}O_{39}^{5-}$ (E^o = ca. 0.15 V) or of $SiW_{12}O_{40}^{4-}$ (E^o = 0.27 V). However, the $H_2OFe^{III}SiW_{11}O_{39}^{5-}$ anion, but not the $SiW_{12}O_{40}^{4-}$ anion, produced a significant decrease in the catalytic current for the reduction of H_2O_2 (Table 3.1). The behavior is consistent with the interception of the hydroxyl radicals generated in the reaction

between $Fe(OH_2)_6^{2+}$ and H_2O_2 by the $Fe^{III}SiW_{11}O_{39}^{5-}$ anion to produce an oxidized intermediate that may either consume H_2O_2 by oxidation or be reduced by a second $Fe(OH_2)_6^{2+}$ ion.

The proposed oxidation by hydroxyl radicals of the Fe(III) centers in $H_2OFe^{III}SiW_{11}O_{39}^{5-}$ is similar to behavior described in a recent pulse radiolytic study of the reaction between OH and $Fe(OH)_4^-$ (14). We therefore carried out analogous experiments in which OH radicals were generated in solutions containing the $H_2OFe^{III}SiW_{11}O_{39}^{5-}$ anions.

Pulse Radiolysis of $H_2OFe^{III}SiW_{11}O_{39}^{5-}$. Solutions of $H_2OFe^{III}SiW_{11}O_{39}^{5-}$ (0.031-2mM) were saturated with N_2O and irradiated with 2 Mev electrons. Under these conditions all e^-_{aq} are converted into OH radicals (vide supra), which react with the iron substituted polytungstate, producing a short-lived species that has an absorption band between 320 and 430 nm (λ_{max} = 355 nm; ε = 8,600 ± 800 M^{-1} cm^{-1}). The growth of the absorbtion was monitored at different wavelengths (320-430 nm.) and used for the computation of the rate constant for this reaction (reaction 1, table 3.2). The rate of the reaction was measured under psuedo first order conditions and found to be first order with respect to both OH radicals and $H_2OFe^{III}SiW_{11}O_{39}^{5-}$ and independent of wavelength.

At the highest concentrations of $H_2OFe^{III}SiW_{11}O_{39}^{5-}$ employed (2mM), the formation of the intermediate was both faster than the competing dimerization reaction of the OH radical ($k(OH + OH \rightarrow H_2O_2) = 5 \times 10^9$ M^{-1} s^{-1}) and complete before its bimolecular decomposition could become significant. The absorbance observed under these conditions

was used to estimate the molar absorbtion coefficients between 400 and 450 nm. Since the spectral data given between 325 and 400 nm. were obtained under conditions where the aforementioned reactions compete significantly, the observed absorbances were normalized utilizing calibration curves (absorbance vs. energy input at varying $H_2OFe^{III}SiW_{11}O_{39}^{5-}$ concentrations). The spectrum has also been corrected for the absorbance of the parent, unreacted, $H_2OFe^{III}SiW_{11}O_{39}^{5-}$ ion, which is given for reference at both pH 4 (fig. 2A) and pH 6.6 (fig. 2B). The spectrum of the intermediate showed no change with pH in the region between 4-7. Studies carried out with the isomorphous $H_2OFeAsW_{11}O_{39}^{4-}$ ion yielded similar kinetic data (see Table 3.3) and a spectrum similar to that in figure 2. Since no spectral changes were observed when similar concentrations of the unsubstituted $SiW_{12}O_{40}^{-4}$ ion were exposed to pulse radiolysis generated OH radicals, it is assumed that the Fe(III) center of the $H_2OFe^{III}XW_{11}O_{39}^{-n}$ ions is the site of OH attack. Hence for purposes of exposition, throughout the chapter we will regard the observed transient derived from the latter complex as a complex of Fe(IV) although this does not exclude the possibility that an OH adduct of Fe(III) is formed instead.

The rate of decomposition of the Fe(IV) intermediate is second order in Fe(IV) and independent of the concentration of $H_2OFe^{III}SiW_{11}O_{39}^{5-}$, when the latter is relatively high (0.125 - 2 mM). At lower $H_2OFe^{III}SiW_{11}O_{39}^{5-}$ concentration the decomposition rate shows an iron dependence as shown in table 3.2.

Hydrogen peroxide yields measured in irradiated N_2O saturated

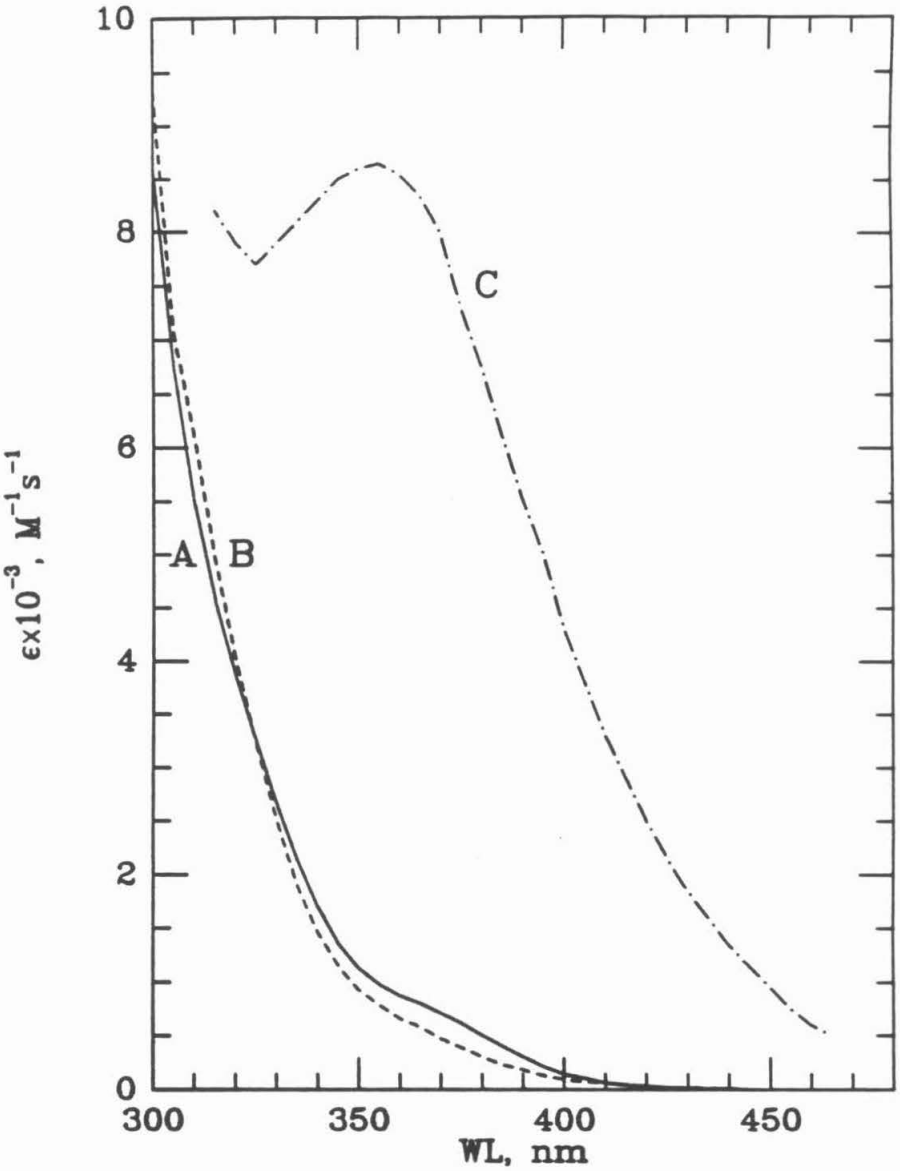

Figure 3.2. Absorbtion spectrum of the transient $HOFe^{IV}SiW_{11}O_{39}^{5-}$(C) formed in reaction of OH radical with $HOFe^{III}SiW_{11}O_{39}^{6-}$ ((A) pH =4; (B) pH =6.6) under pulse radiolysis conditions. Experimental conditions: 0.1 M $NaClO_4$, 2mM. Phosphate, 0.1mM $HOFe^{III}SiW_{11}O_{39}^{6-}$, 0.026 M N_2O, $[OH]_{av}$/pulse 3.3μM, pH 6.6, 24° C.

aqueous solutions in the absence of $H_2OFe^{III}SiW_{11}O_{39}^{5-}$ are in agreement with the expected yields of $G(H_2O_2)_{total} = G(H_2O_2) + 0.5\ G(OH)$. In pulse irradiated N_2O saturated solutions containing $H_2OFe^{III}SiW_{11}O_{39}^{5-}$ at pH 2.4, the $[H_2O_2]$ was very close to that produced in the absence of the $H_2OFe^{III}SiW_{11}O_{39}^{5-}$, strongly suggesting that the decomposition of the Fe(IV) complex produces H_2O_2.

The reduction of $H_2OFe^{III}SiW_{11}O_{39}^{5-}$ by O_2^- was studied at pH 7 and 8 by monitoring the growth of $H_2OFe^{II}SiW_{11}O_{39}^{6-}$ at λ = 450 nm. ($\varepsilon_{450} \approx 200\ M^{-1}cm^{-1}$; see table 3.4 for the conditions and rate data). The O_2^-/HO_2 radicals were generated with a G = 6.1 in O_2 saturated (1.2 mM) formate solutions as described in the experimental section. The formation of the $H_2OFe^{II}SiW_{11}O_{39}^{6-}$ ion was first order in both $H_2OFe^{III}SiW_{11}O_{39}^{5-}$ and O_2^- and yielded bimolecular rates of (1.6 ± 0.3) x $10^3\ M^{-1}\ s^{-1}$ and (3.7 ± 0.7) $M^{-1}\ s^{-1}$ at pH 8 and 7 respectively. The pH dependence of the rate is in the direction expected from the pH dependence of the formal potentials of the $Fe^{III/II}$ couple (1) and therefore the driving force of the reaction. Attempts to measure the rate of the reduction by HO_2/O_2^- at pH 2 proved unsuccessful. Apparently the superoxide that was generated disproportionated at a faster rate than it could reduce the Fe(III) to Fe(II), although the reaction can be complicated by H atoms generated by the reaction of H^+ with e^-_{aq} at this low pH (9).

Steady-state Radiolysis of $H_2OFe^{III}SiW_{11}O_{39}^{5-}$. A ^{60}Co source was utilized to provide continuous radiolysis of solutions saturated with H_2O and containing 0.5 mM $H_2OFe^{III}SiW_{11}O_{39}^{5-}$ and ca. 0.4 mM H_2O_2.

Hydroxyl radicals were generated in the solution at the steady rate of 10^{-7} M s^{-1} (G = 6.0), from which a steady-state concentration of the Fe(IV) complex of ca. 6 x 10^{-9} M can be calculated using the decomposition rate constant in Table 3.2. With these concentrations, almost all of the OH radicals generated during the radiolysis react with the $H_2OFe^{III}SiW_{11}O_{39}^{5-}$ (k_f = 7 x 10^8 M^{-1} s^{-1}) to produce the Fe(IV) anion instead of with the H_2O_2 (k = 4.5 x 10^7 M^{-1} s^{-1} (15)). This system was utilized to examine the reaction of the Fe(IV) complex with H_2O_2. The changes in the H_2O_2 concentration during two different steady state radiolysis experiments are shown in Figure 3.3. Solutions containing H_2O_2 and $H_2OFe^{III}SiW_{11}O_{39}^{5-}$ are stable under these conditions and no change in the concentrations of H_2O_2 was observed in the absence of radiolysis. During the radiolysis H_2O_2 is formed at a low rate by direct recombination of OH radicals in the spur (7). Thus, if the Fe(IV) complex formed in the reaction between the radiolytically generated OH radicals and the $H_2OFe^{III}SiW_{11}O_{39}^{5-}$ anions were stable, a slight increase in the H_2O_2 concentration equal to G = 0.7 would be expected to occur during the radiolysis (7). The expected increase for this case is shown as the dashed line in Figure 3.3. Experimentally, a decrease in the concentration of H_2O_2 was observed, which indicates that the reaction in which an Fe(IV) complex oxidizes H_2O_2 proceeds more rapidly than the second order decomposition of the Fe(IV) anion to produce $H_2OFe^{III}SiW_{11}O_{39}^{5-}$ and H_2O_2. The upper set of points plotted in Figure 3.3 are the experimental concentrations of H_2O_2 measured at pH = 2. The true rate of H_2O_2 disappearance can be calculated by

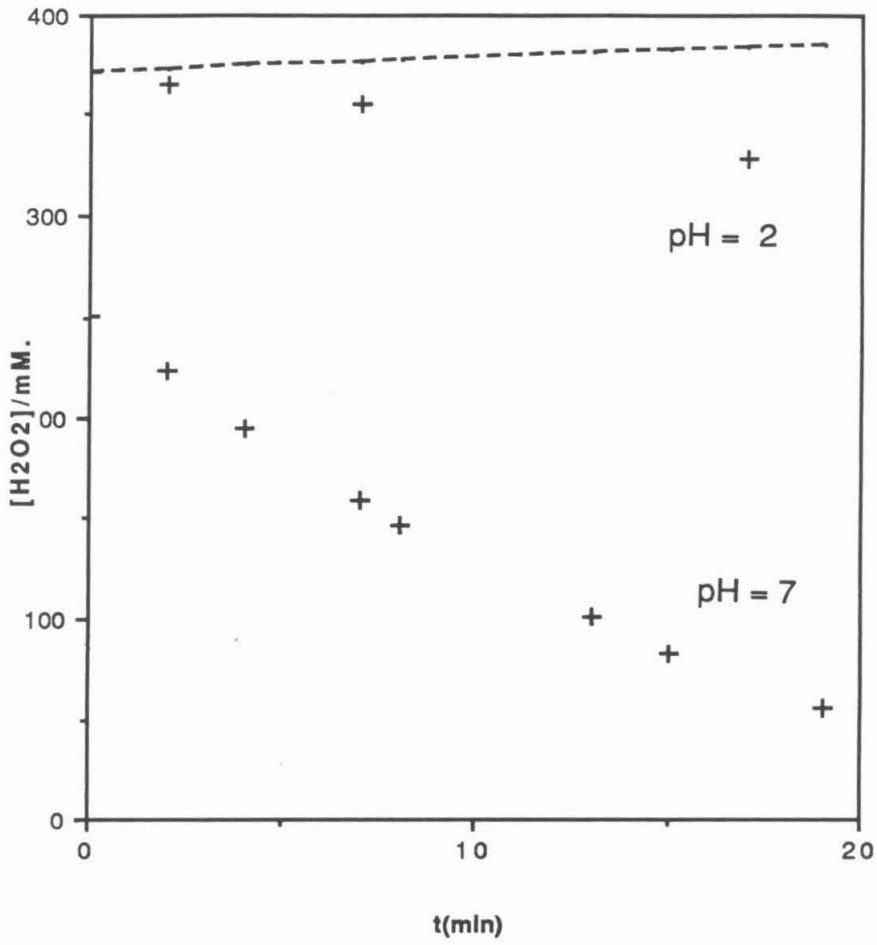

Figure 3.3. Time dependence of the concentration of H_2O_2 in a 0.5 mM solution of $H_2OFe^{III}SiW_{11}O_{39}^{5-}$ during its steady-state radiolysis with a ^{60}Co source. Supporting electrolyte: 0.1 M $NaClO_4$.

correcting the observed rate of disappearance ($G(-H_2O_2)=2.47$) by the known rate of formation of H_2O_2 in the spur (vide supra, $G(H_2O_2)=0.7$) to give a $G(-H_2O_2)$ value of 3.17 This value is close to 1/2 the rate of generation of primary radicals (reaction (1)) under the radiolysis conditions ($G(e^-_{aq} + H + OH) =6.0$).

When the experiment was repeated at pH 5-7, the rate of decrease in the concentration of H_2O_2 was considerably greater, as shown by the lower set of experimental points plotted in Figure 3.3. In fact, the rate of decrease of the H_2O_2 concentration ($G_{initial}(-H_2O_2) \approx 14$) greatly exceeded the rate at which the primary radicals were produced in the radiolysis so that a chain reaction leading to the decomposition of H_2O_2 was indicated at these higher pH values.

DISCUSSION

Basis of the Electrocatalytic Behavior of the $H_2OFe^{III}XW_{11}O_{39}^{n-}$ *Anions.* The catalysis of the electroreduction of H_2O_2 by iron-substituted heteropolytungstates exhibits the hallmarks of an inner-sphere mechanism that requires participation by the iron center. On the cyclic voltammetric time scale, no catalysis is observed with the iron-free parent anion, $SiW_{12}O_{40}^{4-}$, even though this species undergoes a one-electron reduction at a potential very close to that of the one-electron reduction of the catalytically active $H_2OFe^{III}SiW_{11}O_{39}^{5-}$ anion (Figure 3.1). The reduced form of the former anion, $SiW_{12}O_{40}^{5-}$, possesses an electron energetic enough to reduce H_2O_2 but lacks a site for the H_2O_2 to coordinate to the catalyst. The significant catalytic current obtained with the iron-substituted anion

(at the same potential where there is no evidence of catalysis in the voltammogram for the $SiW_{12}O_{40}^{4-}$anion) therefore seems clearly to depend upon an inner-sphere pathway in which the substrate replaces the single, substitutionally labile water molecule in the coordination sphere of the iron center. Additional evidence favoring this description is the observation that the presence of ligands such as pyridine which can compete with H_2O_2 for the coordination site, decreases the magnitude of catalytic currents for the reduction of H_2O_2. Thus, a plausible electrocatalytic mechanism in the presence of excess catalyst is the following:

$$H_2OFe^{III}SiW_{11}O_{39}^{5-} + e^- \rightarrow H_2OFe^{II}SiW_{11}O_{39}^{6-} \quad (2)$$

$$H_2OFe^{II}SiW_{11}O_{39}^{6-} + H_2O_2 \rightarrow H_2O_2Fe^{II}SiW_{11}O_{39}^{6-} + H_2O \quad (3)$$

$$H_2O_2Fe^{II}SiW_{11}O_{39}^{6-} \rightarrow HOFe^{III}SiW_{11}O_{39}^{6-} + OH \quad (4)$$

$$OH + H_2OFe^{II}SiW_{11}O_{39}^{6-} + H^+ \rightarrow H_2O + H_2OFe^{III}SiW_{11}O_{39}^{5-} \quad (5)$$

The order of the initial electron transfer and coordinative displacement steps could be inverted and the final, fast reaction is written as an outer-sphere electron transfer process but could also be written as a hydrogen atom transfer reaction followed by intramolecular electron transfer and protonation.

The mechanism embodied in reactions (2)-(5) requires that two electrons be consumed by each H_2O_2 molecule as is observed in the

presence of excess catalyst. However, under more typical electrocatalytic conditions, where the substrate to catalyst ratio is greater than unity, fewer than two electrons are consumed by each H_2O_2 molecule. These conditions are also those that would favor the participation of the hydroxyl radicals generated in reaction (4) in reactions other than reaction (5) such as the oxidation of the $H_2OFe^{III}SiW_{11}O_{39}^{5-}$ anion. It therefore seems plausible to connect the decrease in the electrons consumed per H_2O_2 molecule with the appearance of the oxidized, Fe(IV) form of the heteropolyanion. The steady-state radiolysis of solutions containing both H_2O_2 and $H_2OFe^{III}SiW_{11}O_{39}^{5-}$ (Figure 3.3) showed that the Fe(IV) form of the heteropolyanion was rapidly reduced by reaction with H_2O_2. This observation provides a possible explanation for the consumption of fewer than two electrons per H_2O_2 molecule during its electroreduction as catalyzed by $H_2OFe^{III}SiW_{11}O_{39}^{5-}$. A reaction sequence that would accommodate this result would be reactions (2) to (4) followed by:

$$H_2OFe^{III}\,SiW_{11}O_{39}^{5-} + OH \rightarrow OFe^{IV}SiW_{11}O_{39}^{6-} + H_2O + H^+ \qquad (6)$$

$$OFe^{IV}SiW_{11}O_{39}^{6-} + H_2O_2 + H^+ \rightarrow H_2OFe^{III}SiW_{11}O_{39}^{5-} + O_2H \qquad (7)$$

$$O_2H \rightarrow 0.5\ O_2 + 0.5\ H_2O_2 \qquad (8)$$

The sum of reactions (2)-(4) plus (6)-(8) yields:

$$1.5\ H_2O_2 + H^+ + e^- \rightarrow 0.5\ O_2 + 2\ H_2O \qquad (9)$$

Only 0.67 electrons are consumed per molecule of H_2O_2 during the catalyzed electroreduction according to this reaction scheme, which is appropriate at pH values below 4 where the superoxide generated in reaction (7) is protonated (10). The number of electrons consumed per molecule of H_2O_2 during an electrolysis will depend on the partitioning of the OH radicals generated in reaction (4) between reactions (5) and (6). Whenever reaction (5) is dominant, the catalyzed electrolysis results in the consumption of two electrons per H_2O_2 molecule just as is obtained if $Fe(OH_2)_6^{3+}$ is employed as the catalyst (5). When reaction (5) proceeds in parallel with reaction (6) followed by reactions (7) and (8), fewer than two electrons per H_2O_2 molecule are consumed. Thus, the observed values of between 0.9 and 2 electrons consumed per molecule of H_2O_2 during its catalyzed electroreduction at the potential of the first reduction wave of the $H_2OFe^{III}SiW_{11}O_{39}^{5-}$ catalyst can be accounted for on the basis of the partitioning of OH radicals between reactions (5) and (6). The simple, two-electron stoichiometry obtained when the electrolysis is carried out at more negative potentials where the catalyst exhibits a two-electron reduction wave, is also understandable because the hydroxyl radicals are then generated in the presence of the Fe(II), not the Fe(III), form of the catalyst and their subsequent rapid reduction by the multiply reduced catalyst avoids the formation of the Fe(IV) complex and involves two electrons per H_2O_2 molecule.

Note that the sum of reactions (6)and (7) yields reaction (10):

$$OH + H_2O_2 \rightarrow O_2H + H_2O \qquad (10)$$

Thus, the same overall stoichiometry leading to the consumption of fewer than two electrons per H_2O_2 molecule would result if the hydroxyl radical produced in reaction (4) oxidized an H_2O_2 molecule instead of an Fe(III) center as in reaction (6). However, the rate of reaction (10) is apparently smaller than that of reaction (6). If this were not the case, the presence of $H_2OFe^{III}SiW_{11}O_{39}^{5-}$ could not have resulted in the observed decrease in the rate of electroreduction of H_2O_2 as catalyzed by $Fe(OH_2)_6^{2+}$ (Table 3.1). The rate constant for reaction (10) is 4.5×10^7 M^{-1} s^{-1} (15). The rate constant estimated for reaction (6) from the pulse radiolysis experiments was 7×10^8 M^{-1} s^{-1}, which is in the proper range to produce partitioning of the OH radicals between reactions (5) and (6) thus accounting for the experimental observations.

Electrocatalysts often achieve their activity through the ability to stabilize high energy intermediates that are inevitably encountered in multiple-electron processes. In the present instance, the high energy species to be stabilized is the hydroxyl radical and the oxidized intermediate that we have depicted as $OFe^{IV}SiW_{11}O_{39}^{6-}$ could be regarded as a (deprotonated) hydroxyl radical stabilized by binding to an Fe(III) center. This viewpoint could be emphasized by replacing reactions (4) and (6) with the concerted, two-electron reaction (11):

$$H_2O_2Fe^{II}SiW_{11}O_{39}^{6-} \rightarrow OFe^{IV}SiW_{11}O_{39}^{6-} + H_2O \qquad (11)$$

The consumption of fewer than two electrons per H_2O_2 molecule during catalyzed electroreductions of H_2O_2 would then be based on the partitioning of the $OFe^{IV}SiW_{11}O_{39}^{6-}$complex between reaction (7) and reaction (12).

$$OFe^{IV}SiW_{11}O_{39}^{6-} + H_2OFe^{II}SiW_{11}O_{39}^{6-} + 2H^+ \rightarrow 2\ H_2OFe^{III}SiW_{11}O_{39}^{5-} \quad (12)$$

As before, the stoichiometry would vary between 0.67 and 2.0 electrons per H_2O_2 molecule as the reaction sequence varied between reactions (2) + (3) + (11) + (7) and reactions (2) + (3) + (11) + (12), respectively.

pH Dependence of H_2O_2 Disappearance During Steady-State Radiolysis. The concentration of H_2O_2 decreased much more rapidly at pH 5-7 than at pH 2 during steady-state radiolysis of N_2O-saturated solutions of $H_2OFe^{III}SiW_{11}O_{39}^{5-}$ (Figure 3.3). This difference seems likely to be associated with the difference in the reactivities of O_2^- and HO_2 (produced in reaction 7) toward $H_2OFe^{III}SiW_{11}O_{39}^{5-}$. The pulse radiolysis of oxygen-saturated formate solutions containing $H_2OFe^{III}SiW_{11}O_{39}^{5-}$ at pH 2 and 7 showed that HO_2/O_2^- readily reduces the Fe(III) center to Fe(II) at pH 7 but not at pH 2. The weaker reducing strength of HO_2 at pH =2 compared with O_2^- at pH =7 (7) makes the reduction of $H_2OFe^{III}SiW_{11}O_{39}^{5-}$ by HO_2 only slightly favored thermodynamically at pH 2 and no reduction was observed during pulse radiolysis at this pH. The HO_2 radicals are probably consumed by disproportionation at pH 2(10) (although the mechanism might be

complicated by the generation of H atoms at this lower pH(11).) This observation suggests that the following chain mechanism, resulting in the catalyzed disproportionation of H_2O_2, operates during the steady-state radiolysis of N_2O-saturated solutions of $H_2OFe^{III}SiW_{11}O_{39}^{5-}$ at pH = 7 under conditions where the initial reaction is between OH and $H_2OFe^{III}SiW_{11}O_{39}^{5-}$ to produce the Fe(IV) form of the heteropolyanion (reaction (6)):

$$OFe^{IV}SiW_{11}O_{39}^{6-} + H_2O_2 \rightarrow H_2OFe^{III}SiW_{11}O_{39}^{5-} + O_2^- \qquad (13)$$

$$H_2OFe^{III}SiW_{11}O_{39}^{5-} + O_2^- \rightarrow H_2OFe^{II}SiW_{11}O_{39}^{6-} + O_2 \qquad (14)$$

followed by reactions (3), (4), and (6), which regenerate the Fe(IV) form of the ion.

The sum of reactions (13) and (14) plus (3), (4), and (6) is:

$$2\ H_2O_2 \rightarrow O_2 + 2\ H_2O \qquad (15)$$

Thus, this reaction sequence can account for the removal of H_2O_2 at a rate greater than the radiolytic generation of OH radicals at pH $\geq$ 5 (Figure 3). Reactions that would interrupt the chain are reactions (5), (8), and (12) as well as:

$$2\ OH \rightarrow H_2O_2 \qquad (16)$$

or

$$O_2^- + OH \rightarrow O_2 + OH^- \qquad (17)$$

The rate constant for all of these chain terminating reactions would be expected to be large. However, all of these reactions are second order in reactants that are present at very low concentrations so that the reaction rates would be relatively small compared with those of the chain propagating reactions ((3), (4), (6), (13), and (14)), which all involve reactants ($H_2OFe^{III}SiW_{11}O_{39}^{5-}$ or H_2O_2) present at much higher concentrations. Thus, it seems plausible that the chain mechanism outlined above is responsible for the enhanced rate of H_2O_2 disappearance during steady-state radiolysis of mixtures of $H_2OFe^{III}SiW_{11}O_{39}^{5-}$ and H_2O_2 at pH 5-7.

Nature of the Complex Formed by One-electron Oxidation of $H_2OFe^{III}SiW_{11}O_{39}^{5-}$. In a recent study of the oxidation of $Fe^{III}(OH)^{4-}$ by hydroxyl radicals, the product was formulated as a ferryl complex, $Fe^{IV}O(OH)_n$ (14). The differences in the spectra of $Fe^{IV}O(OH)n$ and the oxidized species obtained during the pulse radiolysis of $H_2OFe^{III}SiW_{11}O_{39}^{5-}$ in the present study (Figure 3.2), specifically the blue shifting of λ_{max}, might be a result of either the lower pH at which the spectra in this report was obtained or the different coordination environment in which the iron center resides. There is less uncertainty about the coordination environment of the iron center in the present case because the five oxo groups coordinated to the iron center that are also part of the polyoxometallate structure are inert toward substitution. A seven-coordinate Fe(IV) complex formed in an inner-sphere electron transfer reaction to a coordinated OH radical cannot be ruled out, but a more likely reaction pathway would

be hydrogen atom abstraction from the water molecule coordinated to the Fe(III) center by uncoordinated OH radicals. A mechanism involving simple outer-sphere electron transfer to OH is also possible but seems less likely because the rate of the reaction between $H_2OFe^{III}SiW_{11}O_{39}^{5-}$ and OH decreases somewhat when the pH is increased from 4 to 7 (Table 3.1). The formal potential of the Fe^{IV}/Fe^{III} couple almost certainly becomes less positive as the pH increases because of the difference in the degree of protonation at the iron center in the two oxidation states, so that the driving force for the reaction of the Fe(III) center with OH should increase with pH. That the rate decreases instead of increasing with pH, could be regarded as evidence against simple outer-sphere electron transfer and, therefore, would mildly support a hydrogen atom transfer mechanism.

The rate of disappearance of the Fe(IV) complex was dependant on the $H_2OFe^{III}SiW_{11}O_{39}$ concentration. The overall kinetic behavior can be explained by the following mechanism:

$$H_2OFe^{III}SiW_{11}O_{39}^{5-} + OH \rightleftharpoons HOFe^{IV}SiW_{11}O_{39}^{6-} + H_2O \quad (18)$$

$$2\ HOFe^{IV}SiW_{11}O_{39}^{6-} + 2\ H_2O \rightarrow 2\ H_2OFe^{III}SiW_{11}O_{39}^{5-} + H_2O_2 \quad (19)$$

$$HOFe^{IV}SiW_{11}O_{39}^{6-} + OH + H_2O \rightarrow H_2OFe^{III}SiW_{11}O_{39}^{5-} + H_2O_2 \quad (20)$$

where equilibrium (1) lies very far to the right such that over the concentrations range of $H_2OFe^{III}SiW_{11}O_{39}^{5-}$ studied, the reaction is first order in the concentration of $H_2OFe^{III}SiW_{11}O_{39}^{5-}$, yielding k_{18}.

The evidence for the equilibrium is found in the [$H_2OFe^{III}SiW_{11}O_{39}^{5-}$] dependence of the decay rate of the Fe(IV) transient at low $H_2OFe^{III}SiW_{11}O_{39}^{5-}$ concentrations. The predominant pathway for the Fe(IV) disappearance is bimolecular and occurs at the rate found in table 3.2, but the [$H_2OFe^{III}SiW_{11}O_{39}^{5-}$] dependence on the decay rate observed at low [$H_2OFe^{III}SiW_{11}O_{39}^{5-}$] suggests that an equilibrium exists and that the alternative pathways (reactions (20) or possibly (16)) are operative.

Attempts to generate the Fe(IV) complex electrochemically were unsuccessful: No anodic processes were evident in scans to the most positive accessible potentials (1.5 V. vs NHE) with solutions of $H_2OFe^{III}SiW_{11}O_{39}^{5-}$ at the highest pH values at which the complex was stable (pH < 8). Upper and lower limits on the formal potential of the Fe^{IV}/Fe^{III} couple can be estimated on the basis of the observation that the Fe(III) complex is rapidly oxidized by OH and the Fe^{IV} complex is reduced by H_2O_2. For half-reaction (21)

$$OFe^{IV}SiW_{11}O_{39}^{6-} + 2\,H^+ + e^- \rightleftharpoons H_2OFe^{III}SiW_{11}O_{39}^{5-} \qquad (21)$$

these limits are $1.44 < E_f$ (vs NHE) < 2.65 (pH = 0) or $0.61 < E_f < 1.82$ (pH = 7). The failure to observe the anodic oxidation of $H_2OFe^{III}SiW_{11}O_{39}^{5-}$ could be the result of the inaccessibility of a significant portion of this potential range or of the kinetic sluggishness of the electrode process when proton transfer accompanies electron transfer or both.

One of the potentially most interesting aspects of the putative

$OFe^{IV}SiW_{11}O_{39}^{6-}$ complex is its possible utility as a catalyst in oxidation reactions. The high rate constant for the reaction of the oxidized complex with itself (Table 3.2) limits its utility as an oxidation catalyst. The high rate of decomposition of the Fe(IV) complex might explain a recent study in which it was reported that the Co and Mn but not the Fe substituted derivatives of the Keggin ions could act as efficient catalysts for the epoxidation of olefins by oxygen atom donors such as iodosylbenzene (16). If the iodosylbenzene reacts with the Fe substituted Keggin ion to form an Fe(IV) complex, it would probably decompose via reaction (19) before oxidizing the organic substrate. Heteropolytungstates substituted with other oxidizable transition metals are being investigated to determine if longer-lived catalysts can be prepared and exploited.

REFERENCES

1. Toth, J. E.; Anson, F. C., *J. Electroanal. Chem.*, **1988**, *256*, 364.

2. Toth, J. E.; Anson, F. C., *J. Am. Chem. Soc.*, **1989**, *111*, 2444.

3. (a) Zonnevijlle, F.; Tourne, C. M.; Tourne, F. T., *Inorg. Chem.*, **1983**, *22*, 1198. (b) Zonnevijlle, F.; Tourne, C. M.; Tourne, F. T., *Inorg. Chem.*, **1982**, *21*, 2751.

4. (a) Keita, B.; Nadjo, L., *J. Electroanal. Chem.*, **1988**, *247*, 157. (b) Keita, B.; Nadjo, L.; Saveant, J. M., *J. Electroanal. Chem.*, **1988**, *243*, 105. (c) Keita, B.; Nadjo, L., *J. Electroanal. Chem.*, **1988**, *243*, 87. (d) Keita, B.; Nadjo, L., *J. Electroanal. Chem.*, **1988**, *240*, 325. (e) Keita, B.; Nadjo, L.; Haeussler, J. P., *J. Electroanal. Chem.*, **1987**, *230*, 85. (f) Keita, B.; Nadjo, L., *J. Electroanal. Chem.*, **1987**, *227*, 265. (g) Keita B.; Nadjo, L., *J. Electroanal. Chem.*, **1986**, *199*, 229. (i) Keita B.; Nadjo, L., *J. Electroanal. Chem.*, **1985**, 191, 441. (j) Keita B.; Nadjo, L., *J. Electroanal. Chem.*, **1987**, *230*, 267. (k) Keita B.; Nadjo, L., *J. Electroanal. Chem.*, **1987**, *227*, 77. (l) Keita B.; Nadjo, L., *J. Electroanal. Chem.*, **1987**, *219*, 355. (m) Keita B.; Nadjo, L., *J. Electroanal. Chem.*, **1987**, *217*, 287. (n) Keita B.; Lucas, T.; Nadjo, L., *J. Electroanal. Chem.*, **1986**, *208*, 343. (o) Pope, M.T.; Varga, G. M., *Inorg. Chem.*, **1966**, *5*, 1249.

5. (a) Opekar, F.; Beran, Premysl., *J. Electroanal. Chem.*, **1971**, *32*, 49. (b) Skinner, J. F.; Glasel, A.; Hsu, L.; Funt, B. L., *J. Electrochem. Soc.*, **1980**, *127*, 315.

6. Vogel, A., Textbook of Quantitative Analysis, 4th ed., Longman House: London, 1983, p. 355.

7. Schwarz, H. A., *J. Chem. Ed.*, **1981**, *58*, 101.

8. Schuler, R. H.; Patterson, L. K.; Janata, E., *J. Phys. Chem.*, **1980**, *84*, 2089.

9. Buxton, G.V.; Greenstock, C. L.; Hellman, W.P.; Ross, A.B., *J. Phys. Chem. Ref. Data*, **1985**, *17*, 513.

10. Bielski, B. H. J.; Cabelli, D. E.; Arud., R. L.; Ross, A. B., *J. Phys. Chem. Ref. Data*, **1985**, *14*, 1041.

11. Rush, J.D.; Bielski, B.H.J., *J. Phys. Chem.*, **1985**, *89*, 5062.

12. Swallow, A.J. "Radiation Chemistry", **1973**, Longman Group Ltd., London, p. 156.

13. Schwarx, H. A.; Bielski, B.H.J., *J. Phys. Chem.*, **1986**, *90*, 1445.

14. Rush, J. D.; Bielski, B. H. J., *J. Am. Chem. Soc.*, **1986**, *108*, 523.

15. Schwarz, H.A., *J. Phys. Chem.*, **1962**, *66*, 255.

16. Hill, C.L.; Brown, R.B., *J. Am. Chem. Soc.* **1986**, *108*, 536.

TABLE 3.1

Inhibition by $H_2OFe^{III}SiW_{11}O_{39}^{5-}$ of the $Fe(H_2O)_6^{2+}$ Catalyzed Electroreduction of H_2O_2

EXP. NO.	SOLUTION COMPOSITION[a]	ID,μA[b]
1	6m $Fe(H_2O)_6^{2+}$	191[c]
2	1 + 6mM H_2O_2	260
3	2 + 3mM $Fe^{III}SiW_{11}O_{39}^{5-}$	225
4	2 + 3mM $SiW_{12}O_{40}^{4-}$	262

a. Supporting Electrolyte: 0.1M $NaClO_4$ + 0.01M $HClO_4$.

b. Plateau current at a glassy carbon disk electrode rotated at 100 rpm. The current was measured at ca. 0.3 V.

c. Essentially the same plateau current was obtained in the presence of 3mM. $Fe^{III}W_{11}O_{39}^{5-}$ or 3mM $SiW_{12}O_{40}^{4-}$.

TABLE 3.2

The Rate of Reaction of $H_2OFe^{III}SiW_{11}O_{39}^{5-}$ with HO• and the Rate of Decay of $H_2OFe^{IV}SiW_{11}O_{39}^{4-}$ [a]

$[Fe^{III}SiW_{11}O_{39}^{5-}]$,mM	pH	k_6,x$10^{-8}M^{-1}s^{-1}$	k_{19}, x$10^{-9}M^{-1}s^{-1}$
2.0	4		3.02±.09
1.0	4	5.36±0.52	3.27±0.29
0.5	4	4.0±0.42	3.16±0.07
0.25	4	6.4	3.3±0.09
0.125	4	5.2	3.53±0.26
0.062	4	5.0	4.57±0.6
0.031	4	5..8	5.8±0.04
2.0	7	5.35±0.95	2.41±.26
1.0	7	4.73±0.76	2.23±0.20
0.5	7	5.04±0.68	2.09±0.12
0.25	7	4.60±0.48	2.20±0.25
0.125	7	6.3	3.5±0.38
0.062	7	7.0	4.09±0.68
0.5	6.2	5.22±0.60	
0.5	5.9	5.68±0.60	
0.5	5.5	5.62±0.40	
0.5	5.2	5.54±0.70	
0.5	5.0	5.74±0.50	
0.5	4.8	5.78±0.56	
0.5	4.3	6.26±0.84	

a. Experimental Conditions: 0.1M. $NaClO_4$, 2mM. phospate, 26mM. N_2O, 24°C. Estimated errors are based on multiple runs under identical conditions.

TABLE 3.3

The Rate of Reaction of $H_2OFe^{III}AsW_{11}O_{39}^{5-}$ with HO• and the Rate of Decay of $H_2OFe^{IV}AsW_{11}O_{39}^{4-}$ a

$[Fe^{III}AsW_{11}O_{39}^{5-}]$,mM	pH	k_6,x$10^{-8}M^{-1}s^{-1}$	k_{19}, x$10^{-9}M^{-1}s^{-1}$
2.0	4	3.45±0.43	4.64±0.74
1.0	4	3.92±0.39	4.67±0.42
0.5	4	3.50±0.52	4.36±0.33
0.25	4	3.74±0.35	4.24±0.21

a. Experimental Conditions: 0.1M. $NaClO_4$, 2mM. phospate, 26mM. N_2O, 24°C. Estimated errors are based on multiple runs under identical conditions.

TABLE 3.4

The Rate of Reaction of $H_2OFe^{III}SiW_{11}O_{39}^{5-}$ with O_2^-

$[Fe^{III}SiW_{11}O_{39}^{5-}]$,mM	pH	k_{14},$x10^{-3}M^{-1}s^{-1}$
20	7	1.69±0.26
10	7	1.79±0.38
5	7	1.32±0.28
20	8	3.32±0.42
10	8	4.50±0.98
5	8	3.16±0.46

a. Experimental Conditions: 0.1M. formate, 50mM. phospate, 1.2mM. O_2, 24°C. Estimated errors are based on multiple runs under identical conditions.

CHAPTER 4

ELECTROCATALYTIC REDUCTION OF NITRITE AND NITRIC OXIDE TO AMMONIA WITH IRON-SUBSTITUTED POLYOXOTUNGSTATES

ABSTRACT

Heteropolytungstates in which one of the positions normally occupied by a tungsten cation is occupied instead by an iron cation are shown to be catalysts for the electro-reduction of nitrite to ammonia. The lacunary derivatives in which the empty tungsten site is unoccupied show no catalytic activity. The catalytic mechanism involves the intermediate formation of a nitrosyl complex of the Fe(II) form of the catalyst. The pH dependence of the rate of formation of the nitrosyl complex shows that nitrous acid is the reactive form of nitrite between pH 2 and 8. The catalyzed reduction does not produce hydroxylamine as an intermediate and appears to depend on the ability of the multiply reduced heteropolytungstates to deliver electrons to the NO group bound to the iron center in a concerted, multiple-electron step. The iron-substituted heteropolytungstates are not degraded by repeated cycling between their oxidized and reduced states. A particularly valuable feature of the heteropolytungstate is the ease with which the formal potentials of the several redox couples they exhibit can be shifted by changing the identity of the central heteroatom. Exploitation of this feature provides diagnostic information that can be decisive in establishing the mechanism of electrocatalytic processes.

ELECTROCATALYTIC REDUCTION OF NITRITE AND NITRIC OXIDE TO AMMONIA WITH IRON-SUBSTITUTED POLYOXOTUNGSTATES

INTRODUCTION

The efficient electrochemical catalysis of multiple electron processes is an area of continuing interest. The stability of traditional, transition metal complexes that are frequently employed as catalysts is often limited by degradation of the organic ligands that surround the active sites of the catalysts. These organic ligands are often susceptible to oxidation by reactive, radical intermediates, which must be formed along the reaction pathway if the catalyst is capable of transferring only single electrons to the substrate. Approaches that suggest themselves as means to minimize these problems include the design of electrocatalysts that are capable of delivering multiple electrons to a substrate in order to avoid radical intermediates. In addition, catalysts with ligands that are more inert toward oxidizing environments could prove useful. In the hope of developing more robust catalysts we have begun the study of the electrochemical activity of a series of transition metal-substituted heteropolytungstates (1). These compounds consist of a transition metal coordinated to a totally inorganic tungsten-oxo framework that is inert to typical ligand oxidation reactions. It is possible to reduce these complexes reversibly by up to five electrons, which could facilitate the catalysis of multiple electron processes. Thus, these compounds seemed capable of meeting both of the design

criteria mentioned above.

The iron-substituted polyoxoanions that are the subject of this report are derived from the well-known Keggin ions that have the general formula $XW_{12}O_{39}^{m-}$, where X is a tetrahedrally coordinated heteroatom such as silicon that is located in the center of a tungsten-oxo cage (2). In 1966, Baker and co-workers reported that it was possible to substitute various transition metals for one of the tungsten cations and its terminal oxo group located on the periphery of the anion (3). It has since been shown that the tungsten-oxo cage acts as a pentadentate, homoleptic ligand for the incorporated transition metal, with five bridging oxide ions available for coordination (4). The incorporated transition metal typically resides in a pseudo-octahedral environment with one coordination site occupied by a labile water molecule, which can be substituted with other ligands (5-6). Although the parent $XW_{12}O_{39}^{m-}$ compounds have been the subject of numerous electrochemical studies (7-9) the electrocatalytic activity of the transition metal-substituted analogues has yet to be examined, even though the open coordination site of the incorporated transition metal could provide a pathway for inner-sphere electron transfer, which is probably unavailable to the parent $XW_{12}O_{39}^{m-}$ compounds. We were interested in determining if these compounds would exhibit the reactivity of traditional transition metal catalysts combined with the high stability of the polyoxoanions.

The transition metal substituted heteropolytungstates are also attractive because of a very significant diagnostic advantage they offer in examining the mechanisms of electron transfer reactions in

which they participate: The central heteroatom that is imbedded in the center of the multinuclear anion is inaccessible to species in solution and therefore cannot participate directly in reactions that occur at the periphery of the ion. However, changes in the identity of this heteroatom produce systematic changes in the redox potentials of both the transition metal center and the tungsten-oxo cage (1,10). This feature can be exploited to determine the likely site of electrocatalytic activity in the multi-nuclear anions by noting how the potentials where catalyzed electrode reactions proceed are affected by changes in the central heteroatom. The diagnostic value of this tactic is exemplified in this chapter.

The electro-reduction of nitrite ion to ammonia requires a large overpotential at most electrode surfaces, but the reduction can be catalyzed in aqueous solution by various transition metal complexes including iron chelates (11), iron porphyrins (12), and nickel and cobalt cyclams (13). However, with all of these catalysts, hydroxylamine is either the major product or a significant side product and the reduction is believed to occur via a series of one electron steps. This proved to be the case even when N-methyl pyridinium groups were covalently attached to an iron porphyrin in an attempt to obtain a catalyst capable of delivering multiple electrons (12b). By contrast, the iron-substituted heteropolytungstates examined in this study appear to accomplish a multiple-electron reduction of nitrite and nitric oxide to ammonia and other products without the formation of hydroxylamine. In addition, controlled potential electrolyses involving a large number of catalyst turnovers showed

these anions to have excellent long-term durability.

EXPERIMENTAL

Materials. Unsubstituted and iron-substituted heteropolytungstates were prepared as the α isomers and purified as described previously (5a). Gaseous nitric oxide was passed through a short column of KOH prior to use to remove any acidic impurities. Deionized water was further purified by passage through a purification train (Barnsted-Nanopure). Prepurified argon was deoxygenated by passage through acidic solutions of V(II). All other chemicals were reagent grade and used as received. 0.1 M buffer solutions were prepared by partial neutralization of the following acids: HSO_4^- (pH 2); Cl_3COOH (pH 2.5-3); CH_3COOH (pH 3.5-6.0); morpholinoethanesulfonic acid, MES (pH 6-7); hydroxyethylpiperazinesulfonic acid, HEPES (pH 7-8).

Solutions of the reduced (Fe(II)) forms of the heteropolytungstates were prepared by controlled potential electrolyses of solutions of the Fe(III) forms and were handled under argon using standard Schlenk line techniques. Solutions of the air sensitive nitrosyl complexes could be obtained either by exhaustive controlled potential electrolysis of equimolar amounts of the Fe(III) substituted ions and nitrite ions at potentials just negative of the peak potential of the Fe^{III}/Fe^{II} couples, or by saturation of Fe(II) solutions with NO gas for ca. three minutes. Solutions prepared by either technique displayed identical spectral and chemical properties. Tetra-n-butyl ammonium salts of the nitrosyl complexes were isolated by precipitation with tetra-n-butyl ammonium bromide at pH 4 and were handled in a drybox.

KBr pellets containing the air sensitive nitrosyl complexes were prepared in a drybox and sandwiched on both sides with pure KBr to limit oxygen exposure while the spectra were being recorded.

Apparatus and Procedures. Electrochemical measurements were conducted under argon in conventional two- and three-compartment cells with a glassy carbon working electrode, platinum wire counter electrode and a sodium chloride-saturated calomel reference electrode (SSCE). Formal potentials for reversible couples were taken as the average of anodic and cathodic peak potentials. The working electrode (0.20 cm^2) was polished with 0.3 micron alumina and washed with purified water before use. A combination of Princeton Applied Research instrumentation was used to record cyclic voltammograms and to conduct controlled potential electrolyses at stirred mercury pool electrodes. During unusually extensive electrolyses, small quantities of deoxygenated acetic acid were injected into the cell if the pH of the buffer solutions began to change.

Uv-vis spectra were recorded on a Hewlett-Packard Model 8450A spectrophotometer. Kinetic runs were performed on this spectrophotometer or with a Durham model D110 stopped-flow spectrophotometer equipped with a Tektronix Model 5223 storage oscilloscope. Sodium nitrite and $H_2OFe^{II}XW_{11}O_{39}^{(n+1)-}$ solutions were prepared fresh daily. Standardization of the nitrite solutions with permanganate (15) revealed that there was no decomposition over the course of several hours. All kinetic runs were carried out at constant ionic strength (0.1 M) and under pseudo first order conditions with nitrite present in at least a ten-fold excess. The

extent of reaction was typically followed at two wavelengths: near 460 nm, where the nitrosyl complexes have maxima, and near 700 nm, where the $Fe^{II}XW_{11}O_{39}^{(n+1)-}$ complexes absorb strongly. Pseudo first order rate constants were obtained from plots of ln (A-Ao) vs. time.

Electrolysis solutions were analyzed for ammonia as ammonium cation by ion chromatography (Dionex Model 2020i). Hydroxylamine was determined as the indoxine after reaction with 8-quinolionol in solutions freed of any gaseous, nitrogen-based products (*i.e.*, NO, N_2, N_2O) by purging with air for 10 minutes and adjusting the solution pH to 7 (16). The concentration of indooxine was measured spectrophotometrically at pH 6.8 at λ = 706 nm; ε = 4.3 x 10^3 (16). Blank runs revealed that ammonium, nitrite, nitrate, and acetate ions, and the various iron-substituted heteropolytungstates did not interfere with the procedure. As a check, known amounts of hydroxylammonium chloride were added to electrolysis solutions and the analysis procedure repeated. In no case was any interference observed by any of the species present in solution after electrolyses.

Infrared spectra of the nitrosyl complexes were recorded on a Beckman Instruments Model 4240 IR Spectrometer.

RESULTS

Electrochemical Response of the Heteropolyanions. Four iron-substituted heteropolytungstates were examined in this study: $H_2OFe^{III}XW_{11}O_{39}^{n-}$ (X = Si or Ge, n = 5; X = As or P, n = 4). Their basic electrochemistry in the absence of reducible substrates has been described recently (1). $H_2OFeSiW_{11}O_{39}^{5-}$, $H_2OFeGeW_{11}O_{39}^{5-}$, and

$H_2OFePW_{11}O_{39}^{4-}$ are stable between pH 2 and 8. $H_2OFeAsW_{11}O_{39}^{4-}$ is stable between pH 2 and 6. The three cyclic voltammograms in Figure 4.1 contrast the behavior of one of the unsubstituted parent anions, $SiW_{12}O_{39}^{4-}$, the lacunary anion obtained by removal of one tungsten cation and its terminally bound oxo group, $SiW_{11}O_{39}^{8-}$, and the iron-substituted anion, $H_2OFeSiW_{11}O_{39}^{5-}$. The voltammogram for $SiW_{12}O_{39}^{4-}$ in the potential range of interest consists of two, reversible, one-electron waves followed by a reversible two electron wave (7-9) (Figure 4.1A). Removal of the tungsten-oxo group to produce the lacunary anion leads to a voltammogram with two, reversible, two-electron waves (Figure 4.1B). When an iron(III) center is substituted into the vacant site of the lacunary ion a new, reversible, one-electron wave appears at a more positive potential and the positions of the pair of two-electron waves of the lacunary ion are shifted slightly. The new, one-electron wave has been assigned to the reduction of the bound iron(III) to iron(II) (1,5) and the two-electron waves at more negative potentials to the reduction of tungsten centers in the polyoxometallate framework. Controlled potential electrolysis of the iron-substituted anion at ca. -350 mV consumes one electron and produces very darkly colored solutions which exhibit an extremely broad and featureless absorption that spans essentially the entire visible portion of the spectrum (ε = 200 M^{-1} cm^{-1} at λ = 500 nm). These reduced solutions are air-sensitive but appear stable indefinitely under anaerobic conditions. The formal potentials of the iron-based waves depend upon the identity of the central heteroatom (see Table 4.1) as well as the pH and ionic

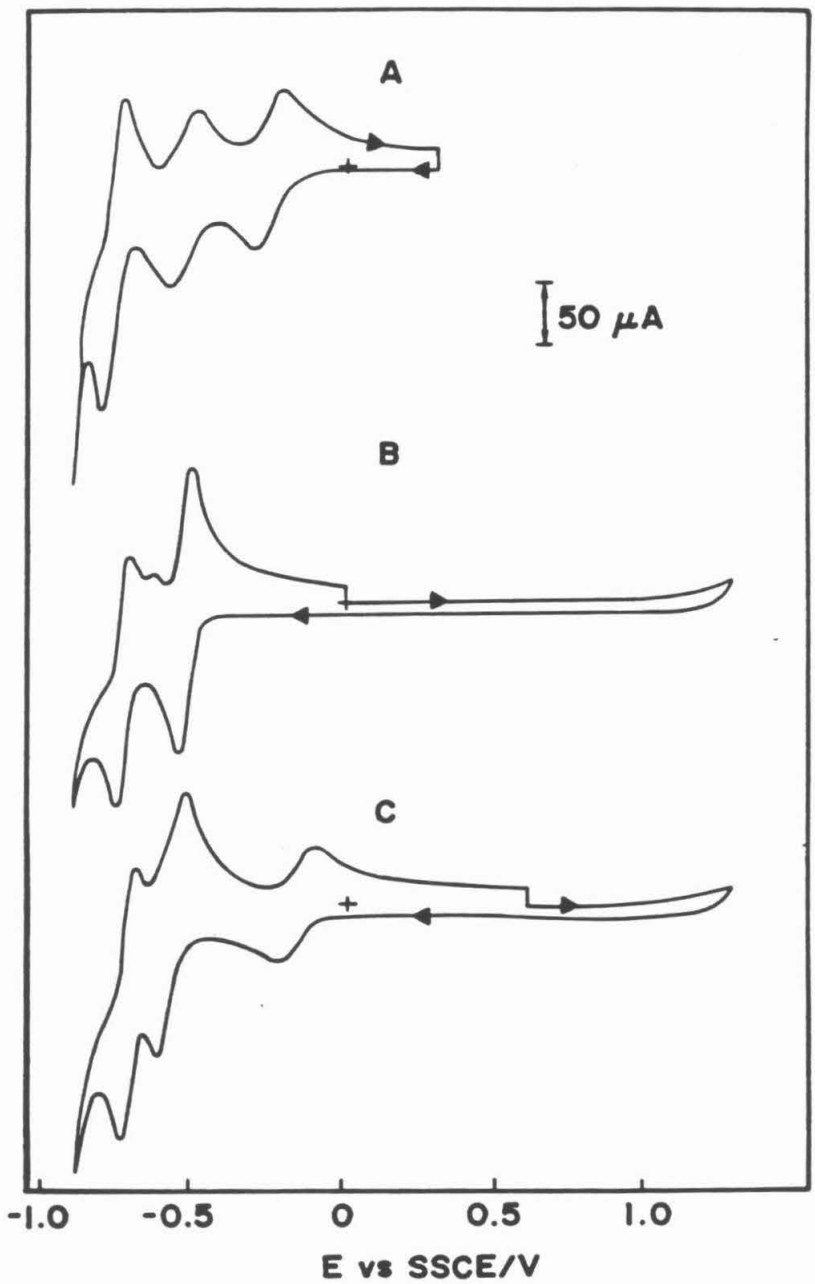

Figure 4.1. Cyclic voltammetry of 1 mM solutions of silicon polytungstate anions at a glassy carbon electrode. (A) $SiW_{12}O_{39}^{4-}$; (B) $SiW_{11}O_{39}^{8-}$; (C) $FeSiW_{11}O_{39}^{5-}$. Supporting electrolyte: 0.1 M $NaClO_4$ + 0.01 M $HClO_4$. Scan rate = 50 mV s^{-1}.

strength (1).

Formation of Iron(II) Nitrosyl Complexes. Addition of an equimolar quantity of $NaNO_2$ to a solution of $H_2OFe^{III}SiW_{11}O_{39}^{5-}$ produces no changes in the spectrum of the solution indicative of a reaction between the two anions. However, there are significant changes in the voltammetry of the mixed solution as shown in Figure 4.2. At pH 2 the cathodic peak current of the first, iron-based wave is enhanced while its anodic counterpart is greatly diminished and the two two-electron waves at more negative potentials are also greatly enhanced (Figure 4.2A). It seems clear that the reduced forms of the heteropolyanion react with the added nitrite. As the pH increases, the enhancement of the current at potentials corresponding to the Fe^{III}/Fe^{II} couple decreases. For example, at pH 5 the addition of nitrite is virtually without effect on the Fe^{III}/Fe^{II} response (Figure 4.2B). However, the two-electron reduction waves of the $H_2OFe^{II}SiW_{11}O_{39}^{6-}$ anion that appear at more negative potentials are still significantly enhanced by the addition of nitrite (Figure 4.2C) so that at pH 5 the reduction of nitrite appears to be catalyzed by the multiply reduced but not the singly reduced forms of the iron-substituted heteropolytungstate. The presence of the iron center is essential for the catalysis because nitrite is without effect on the voltammetry of the lacunary derivative, $SiW_{11}O_{39}^{8-}$, despite the fact that this anion exhibits voltammetric responses at potentials similar to, or even more negative than, those of the $H_2OFe^{III}SiW_{11}O_{39}^{5-}$ anion (Figure 4.2D). Although the catalytic rate decreases significantly as the pH is increased, most of the experiments were conducted at pH 4 or above in order to

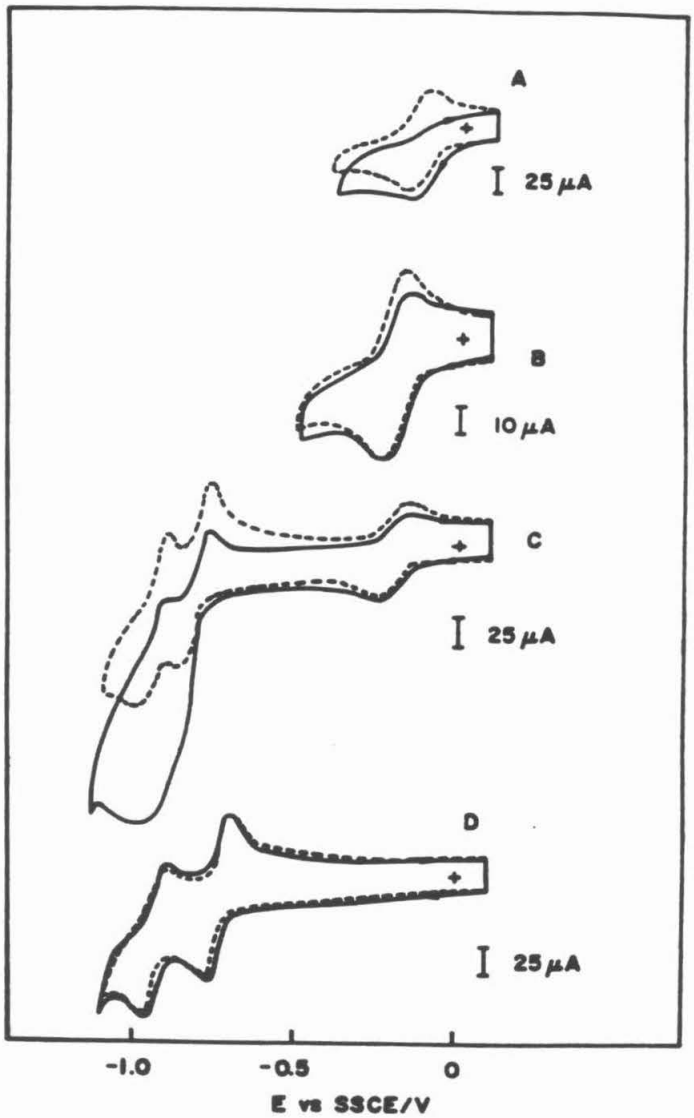

Figure 4.2. Cyclic voltammogram of 1 mM solutions of $Fe^{III}SiW_{11}O_{39}^{5-}$ (A-C) and $SiW_{11}O_{39}^{8-}$ (D) before (----) and after (———) addition of 1 mM NO_2^-. (A) Scan restricted to the Fe^{III}/Fe^{II} couple; supporting electrolyte: 0.1 M $NaHSO_4^-/Na_2SO_4$ at pH 2. (B) As in A; supporting electrolyte: 0.1 M CH_3COONa/CH_3COOH at pH 5. (C) The entire wave; supporting electrolyte as in B. (D) The lacunary anion; supporting electrolyte as in B. Scan rate = 50 mV s^{-1}.

avoid complications associated with the possible disproportionation of HNO_2 (17).

Controlled potential reduction of equimolar mixtures of NO_2^- and $H_2OFe^{III}SiW_{11}O_{39}^{5-}$ at -400 mV in solutions buffered at pH 4 consumes 2 electrons per heteropolyanion and yields a pale red solution that contains an Fe^{II}-NO adduct (vide infra). The iron-substituted heteropolytungstates with Ge, P, and As as heteroatoms behave similarly when the iron center is reduced in the presence of nitrite.

The coulometry at a reduction potential of -400 mV is consistent with the following reaction sequence

$$2\ H_2OFe^{III}SiW_{11}O_{39}^{5-} + 2e \rightarrow 2H_2OFe^{II}SiW_{11}O_{39}^{6-} \quad (1)$$

$$2\ H_2OFe^{II}SiW_{11}O_{39}^{5-} + NO_2^- + 2H^+ \rightarrow ONFe^{II}SiW_{11}O_{39}^{6-} + H_2OFe^{III}SiW_{11}O_{39}^{5-} + 2H_2O \quad (2)$$

in which one Fe(II) center reduces the NO_2^- to NO, which coordinates to the second Fe(II) center in the labile site normally occupied by a water molecule.

The absorption spectra of the reduced solutions have a maximum that varies between 460 and 470 nm depending on the identity of the central heteroatom. The spectra resemble that of the well characterized ONFe(edta) complex (edta = ethylenediaminetetaacetate) for which λmax = 440 nm (18). Infra-red spectra of the insoluble tetra-n-butylammonium salts of the complexes, prepared by reduction of the Fe(III) center in the presence of nitrite, were measured in KBr disks

protected from atmospheric oxygen (see Experimental). A prominent band assignable to an NO stretching mode (19) was observed near 1750 cm^{-1}. The exact position of the band varied with the formal potential of the Fe^{III}/Fe^{II} couple in a manner that is consistent with this assignment (Table 4.1), *i.e.*, the more strongly reducing complexes exhibited the weaker nitrogen-oxygen bonds expected from back donation into π^* orbitals of the coordinated NO.

Complexes with spectra identical to those prepared electrochemically by reduction of $H_2OFe^{III}XW_{11}O_{39}^{n-}$ in the presence of NO_2^- can also be prepared by direct reaction between gaseous NO and the reduced $H_2OFe^{II}XW_{11}O_{39}^{(n+1)-}$ anions. The pale red NO adduct prepared in this way is converted to the original $H_2OFe^{II}XW_{11}O_{39}^{(n+1)-}$ anion when NO is removed from the solution by argon bubbling for ca. 15 minutes. Such reversible formation of a nitrosyl adduct has also been reported for Fe^{II}(edta) and related complexes (18). Addition of NO to solutions of the unreduced Fe(III) forms of the heteropolytungstates produced no evidence of reaction.

Kinetics of Formation of Nitrosyl Adducts. The reaction between $H_2OFe^{II}XW_{11}O_{39}^{(n+1)-}$ anions and nitrite to form the nitrosyl complex proceeds cleanly and at an easily measured rate. The large spectral changes associated with the reaction, shown in Figure 4.3 for the representative $H_2OFe^{II}GeW_{11}O_{39}^{6-}$ anion at pH=7, facilitated the measurement of reaction rates spectrophotometrically. The reaction rate is first order with respect to total nitrite and to the concentration of the heteropolytungstate anion. The rate is also pH dependent as shown in Figure 4.4. The observed second order rate

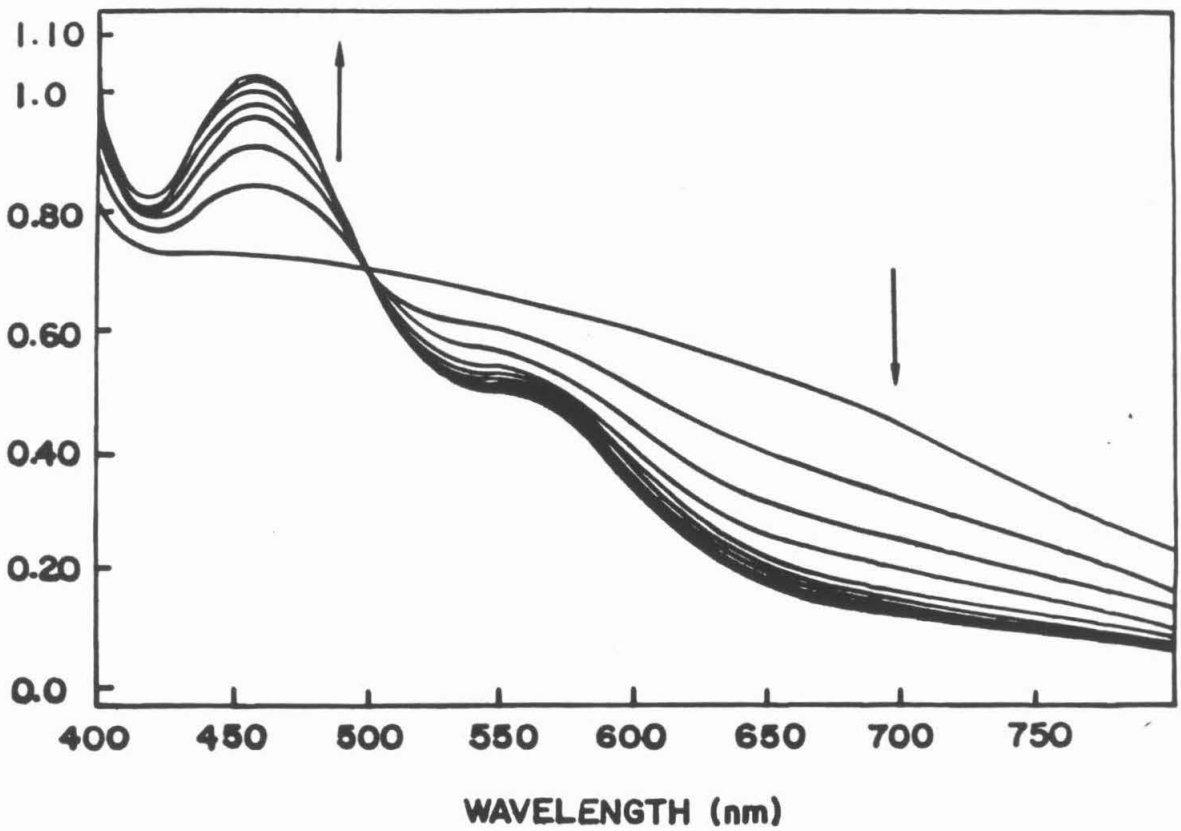

Figure 4.3 Absorption spectra of a mixture of $Fe^{II}GeW_{11}O_{39}^{6-}$ and NO_2^- at pH = 7. Spectra were recorded at 8 minute intervals. Initial concentrations: $Fe^{II}GeW_{11}O_{39}^{6-}$ ca. 2 mM; NO_2^-, 40 mM.

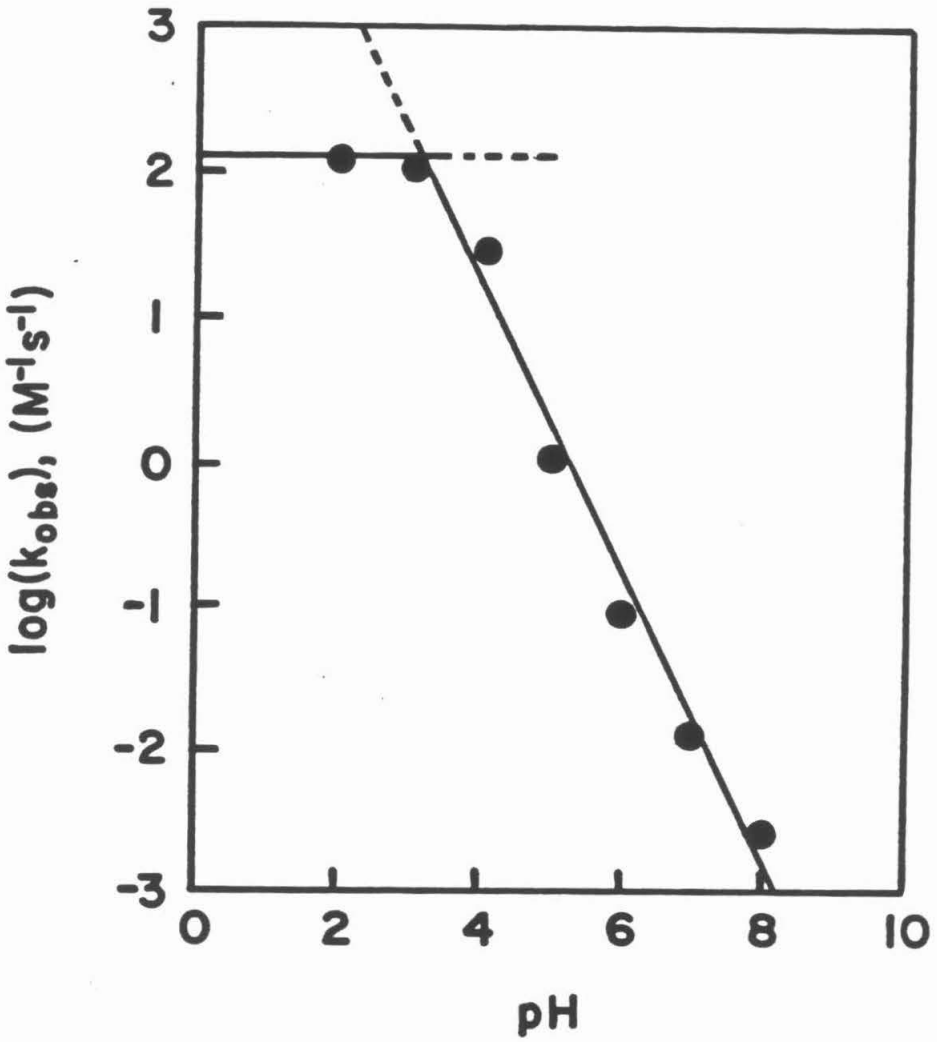

Figure 4.4. pH dependence of the second order rate constants for the reaction of $Fe^{II}GeW_{11}O_{39}^{6-}$ with NO_2^- as obtained from spectral data such as those in Figure 4.3. k_{obs} is the measured pseudo-first order rate constant divided by the analytical concentration of nitrite.

constant, k_{obs}, is proportional to the proton concentration between pH 4 and 8 (the slope of a linear least squares fit to the data points between pH 4 and 8 is 0.998) and becomes essentially independent of pH between pH 4 and 2. The intersection of the horizontal line in Figure 4.4 with the least squares line drawn through the measured values of k_{obs} at pH > 4 occurs at pH = 3.3, which is the pKa of HNO_2. Thus, the kinetic data point to HNO_2 as the reactive form of nitrite in the reaction being monitored (20). The rate constants obtained for the four heteropolyanions are listed in Table 4.1. The particular reactions whose rates we believe are governed by these rate constants will be specified in the Discussion section.

Electrochemistry of $ONFe^{II}XW_{11}O_{39}^{(n+1)-}$. To avoid complications from the electroactivity of the NO and NO_2^- ligands themselves, it is convenient to prepare solutions of $ONFe^{II}XW_{11}O_{39}^{(n+1)-}$ complexes by reacting NO with $H_2OFe^{II}XW_{11}O_{39}^{(n+1)-}$ and quickly removing the excess NO by bubbling argon through the solution for a few minutes and then over the surface of the solution. The resulting complexes appear spectrally identical to those prepared in the presence of excesses of NO_2^- or NO and their dissociative decompositions proceed sufficiently slowly to allow their electrochemistry to be examined in the absence of significant free ligand.

Curve A in Figure 4.5 is a cyclic voltammogram for a solution of $H_2OFe^{II}SiW_{11}O_{39}^{6-}$ prepared by electrolysis of the Fe(III) derivative. The assignment of the three waves has been discussed in connection with Figure 4.1. The voltammogram in curve B was obtained after the solution was saturated with NO for 3 minutes followed by the rapid

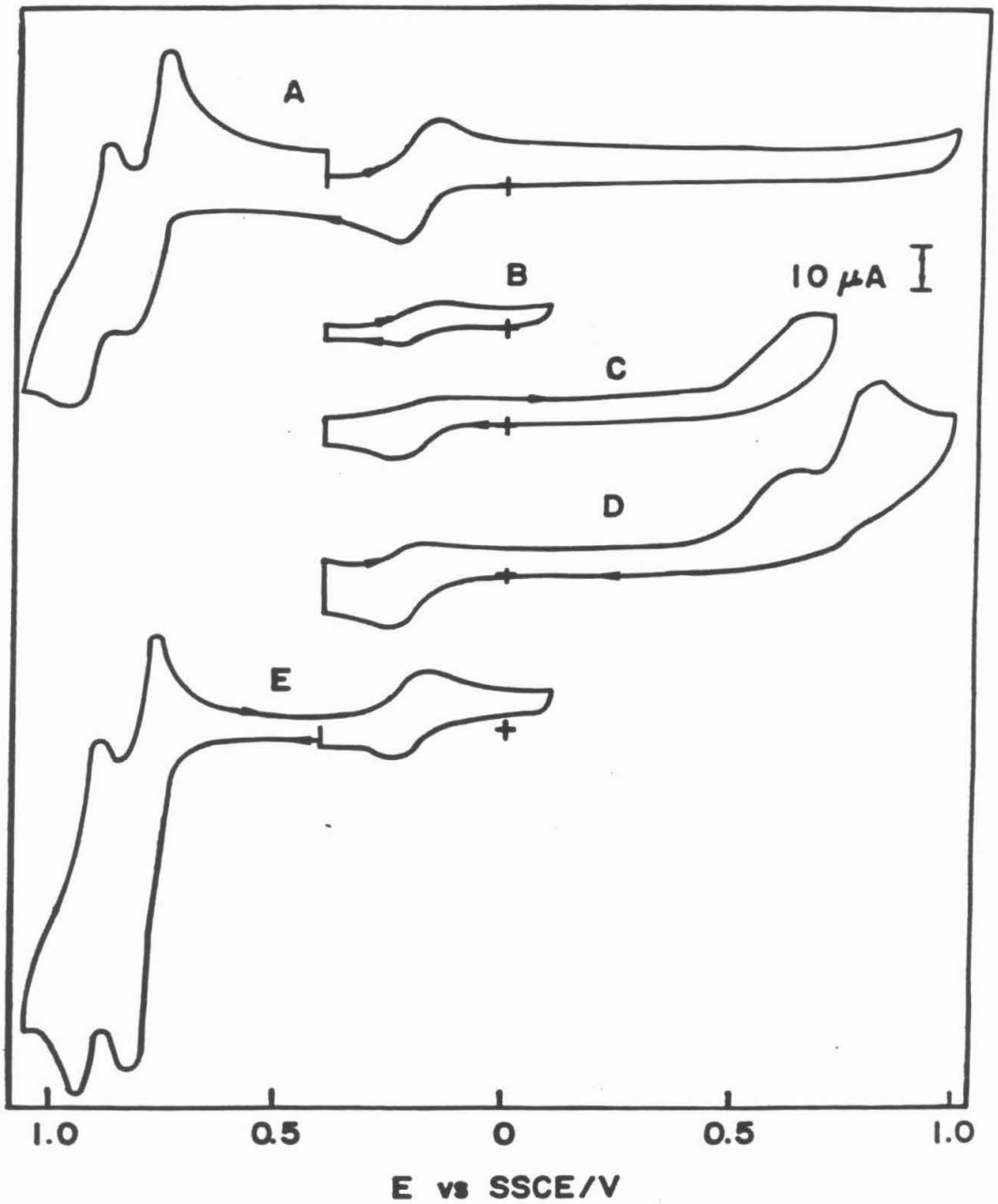

Figure 4.5. Cyclic voltammetry of 1 mM $Fe^{II}SiW_{11}O_{39}^{6-}$ before (A) and after (B-E) formation of $ONFe^{II}SiW_{11}O_{39}^{6-}$ by bubbling with NO followed by rapid purging with argon. Supporting electrolyte: 0.1 M CH_3COONa/CH_3COOH at pH 4.5. Scan rate = 50 mV s^{-1}.

removal of excess NO as described above. The response arising from the Fe^{III}/Fe^{II} couple in the heteropolyanion is much diminished because NO is coordinated to most of the Fe centers, which produces a large positive shift in their oxidation potential, as expected for significant back donation into the low-lying π^* orbitals of the NO. Extension of the potential scan to more positive potentials revealed two new, irreversible anodic peaks between 700 and 1000 mV (curve 4.5D). The first new wave consumed more than one electron per iron center and seems likely to represent a composite oxidation of Fe(II) to Fe(III) and of the coordinated NO to NO_2^-. During the return scan the presence of the original Fe(III) center was revealed by the increase in the cathodic peak current at ca. -150 mV. The second new anodic peak in curve 4.5D appeared at the same position where the oxidation of NO_2^- to NO_3^- was observed in separate experiments in the same supporting electrolyte in the absence of any heteropolyanion.

Repetition of the experiment of Figure 4.5D with the germanium complex, $ONFe^{II}GeW_{11}O_{39}^{6-}$, produced a positive shift of 100 mV in the first new anodic peak. The same positive shift also occurs in the formal potential of the Fe^{III}/Fe^{II} couple in the corresponding parent complex, $H_2OFe^{III}GeW_{11}O_{39}5-$, (Table 4.1). The second new anodic peak in solutions of the $ONFe^{II}GeW_{11}O_{39}^{6-}$ complex appeared at the same position as the second new anodic peak of the $ONFe^{II}SiW_{11}O_{39}^{6-}$ complex as expected for a wave arising from the oxidation of uncoordinated NO_2^- to NO_3^-.

Experiments with the corresponding As and P heteropolyanions produced similar results except that a further positive shift in the

first new anodic peak caused the two anodic peaks to merge. Cycling the potential over the merged peaks produced the same increase in the Fe^{III}/Fe^{II} response near -150 mV that occurred with the other complexes.

Examination of the voltammetry of the nitrosyl complexes in the vicinity of the waves corresponding to the reduction of the tungsten cage in the parent, iron-substituted heteropolyanion revealed large enhancements in the reduction currents (curve E, Figure 4.5). Scanning the potential over the enhanced cathodic peaks led to the reappearance of the Fe^{III}/Fe^{II} response at -150 mV on the return scan, indicating that the unsubstituted parent complex, $H_2OFe^{III}SiW_{11}O_{39}^{6-}$, is generated during the cathodic cycle. Changing the central heteroatom of the heteropolyanion produced shifts in the reduction waves for the nitrosyl complexes similar to those observed for the tungsten-based waves of the parent complexes.

Controlled Potential Electrolytic Reductions. Electrolysis of solutions containing mixtures of $H_2OFe^{III}XW_{11}O_{39}^{n-}$ and NO_2^- at stirred, mercury pool electrodes maintained at potentials negative of the second, two-electron, cathodic wave (*e.g.*, 900 mV) proceeded in two stages. Early in the electrolysis the pale red color of the nitrosyl complex developed just as it did when the electrolysis was conducted at potentials just negative of the first, one-electron wave (vide supra). However, as the electrolysis continued, much larger quantities of charge were consumed and the solution eventually turned the deep blue color characteristic of highly reduced heteropolyanions. Analysis of the resulting solution revealed that significant

quantities of NH_4^+ had been produced.

The efficiency of the catalytic electro-reduction of nitrite to ammonia was examined by conducting a series of controlled potential electrolyses under varying experimental conditions. With catalyst/nitrite ratios of unity or greater, it was possible to reduce most of the nitrite present to ammonia with high faradaic efficiency. In one experiment the electrolysis was carried out in two stages: First the potential was maintained at -300 mV where the NO_2^- was converted quantitatively to the nitrosyl complex, $ONFe^{II}XW_{11}O_{39}^{(n+1)-}$. During this stage no ammonia could be detected in the solution. In the second stage the potential was adjusted to 900 mV, where the generation of ammonia commenced as the nitrosyl complex was reduced.

Experiments conducted under more realistic catalytic conditions, with catalyst-to-nitrite ratios much less than one, produced the results summarized in Table 4.2. The quantity of charge consumed depended on the identity of the heteroatom present in the catalyst despite the very similar formal potentials of the processes corresponding to reduction of the tungsten-oxo framework for all of the catalysts (1). The reasons for the variations in charge consumed are not clear although catalyzed hydrogen evolution by slow modification of the electrode surface as described by Nadjo and co-workers (9 a-i) is one possibility. Analysis of the solutions at the point in the electrolysis where the first permanent blue color appeared (corresponding to an excess of multiply reduced catalyst) revealed the presence of substantial quantities of ammonia. The coulombic efficiencies with which the ammonia was generated are listed

in Table 4.2. It seems clear that both the identity of the central heteroatom and the ratio of catalyst to nitrite affect the amount of ammonia generated. We did not attempt to identify the other products of the catalyzed electroreduction quantitatively. However, the otherwise stable, nitrosyl complexes of the heteropolytungstate catalysts, $ONFe^{II}XW_{11}O_{39}^{(n+1)-}$, were observed to react with excess NO_2^- to yield what appeared to be NO and oxidized catalyst. With the large excesses of NO_2^- present in the experiments of Table 4.2, the NO generated in this way might well have escaped with the flowing argon from the unsealed reaction solution. (The aqueous solubility of NO is only 2 mM at one atmosphere pressure (22).) This could account for the decrease in the quantity of ammonia generated as the ratio of nitrite to catalyst increased, and for the disappearance of all of the nitrite upon the consumption of as little as 1.8 electrons per nitrite ion (Experiment 6 in Table 4.2).

Nitrite might also be consumed without the consumption of faradaic charge via reaction (3) (17):

$$3\ HNO_2 \rightleftharpoons NO_3^- + 2\ NO + H^+ + 2\ H_2O \qquad (3)$$

Permanganate titrations of solutions of NO_2^- in the supporting electrolytes employed showed that there was negligible loss on the time scale of typical electrolyses (ca. 2 hr.). However, in the presence of the oxidized forms of the heteropolyanions, $H_2OFe^{III}XW_{11}O_{39}^{n-}$, some loss of NO_2^- occurred (ca. 10% in 2 hours) and NO_3^- was detected in the solution. Thus, the $H_2OFe^{III}XW_{11}O_{39}^{n-}$

anions may be mild catalysts for reaction (3).

The possibility that hydroxylamine is generated during the electrolysis was examined in Experiment 5 of Table 4.2 by halting the electrolysis about half way to completion where ca. 200 electrons per catalyst molecule had been consumed. Analysis of the electrolysis solution revealed the presence of only a small quantity of hydroxylamine (6.5×10^{-5} M) but a substantial quantity of ammonia. Since it was established in separate experiments that hydroxylamine is a much less reactive substrate than NO_2^- or NO (see figure 4.6), these results indicate that if hydroxylamine is formed during the catalyzed reduction of nitrite to ammonia it is further reduced more rapidly than it can escape from the the substrate-catalyst complex.

DISCUSSION

The results described above have identified several steps in the chemistry that ensues when nitrite is exposed to the $H_2OFe^{II}XW_{11}O_{39}^{(n+1)-}$ complexes.

Formation and Reactivity of Nitrosyl Complexes. The formation of nitrosyl complexes by reaction of nitrite with complexes of Fe(II) is well known (12,18) although the kinetics of the process have not been investigated extensively. The pH dependence of the cleanly second order rate constant (k_{obs}) for the formation of the complexes with heteropolytungstates as shown in Figure 4.4 is compatible with a mechanism in which $H_2OFe^{II}XW_{11}O_{39}^{(n+1)-}$ reduces HNO_2 to NO followed by the rapid coordination of NO by a second molecule of

$H_2OFe^{II}XW_{11}O_{39}^{(n+1)-}$. Although the reduction step could, in principle, involve outer-sphere electron transfer, the alternative mechanism expressed in Scheme 4.1 that features an inner-sphere electron transfer step seems preferable.

Scheme 4.1:

$$NO_2^- + H^+ \rightleftharpoons HNO_2 \quad (4)$$

$$HNO_2 + H_2OFe^{II}XW_{11}O_{39}^{(n+1)-} \rightleftharpoons HNO_2Fe^{II}XW_{11}O_{39}^{(n+1)-} + H_2O \quad (5)$$

$$HNO_2\ Fe^{II}XW_{11}O_{39}^{(n+1)-} \rightarrow HOFe^{III}XW_{11}O_{39}^{(n+1)-} + NO \quad (6)$$

$$H_2OFe^{II}XW_{11}O_{39}^{(n+1)-} + NO \rightleftharpoons ONFe^{II}XW_{11}O_{39}^{(n+1)-} + H_2O \quad (7)$$

$$HOFe^{III}XW_{11}O_{39}^{(n+1)-} + H^+ \rightleftharpoons H_2OFe^{II}XW_{11}O_{39}^{n-} \quad (8)$$

Reactions (4) and (5) are fast pre-equilibria, reaction (6) is the rate determining step and reactions (7) and (8) are fast follow-up steps. There are several reasons that we prefer Scheme 4.1 over the corresponding outer-sphere pathway: 1) The strongly reducing lacunary anions, $XW_{11}O_{39}^{(n+3)-}$, which lack a suitable coordination site for HNO_2 (or NO_2^-) do not reduce HNO_2 (or NO_2^-) at an appreciable rate despite their much more negative formal potentials (Fig. 4.2D). 2) Assuming that the equilibrium constant for reaction (5) is not large,

the driving force for reaction (6) is considerably greater than that of the corresponding outer-sphere reaction (which would yield uncoordinated hydroxide ion) because of the affinity of the iron(III) center for hydroxide ion. For example, in the case of X = Si the driving force advantage for the inner-sphere pathway amounts to ca. 450 mV because K_8 is only $2x10^6$ M^{-1} (1). 3) Voltammograms of equimolar mixtures of NO_2^- and $H_2OFe^{III}XW_{11}O_{39}^{(n-1)-}$ at pH 5 or above show no evidence of a catalytically enhanced reduction at potentials corresponding to the Fe^{III}/Fe^{II} couple (Figure 4.2B). This behavior is in accord with the rate constants listed in Table 4.1 for the formation of the nitrosyl complexes that correspond to negligible formation of the complexes during the time required to record the voltammograms in Figure 4.2C. However, at the more negative potentials where reduction of the tungsten-oxo framework occurs, significant catalytic currents are observed (Figure 4.2C). Coordination of NO to the reduced iron center has been shown to be a prerequisite for its catalytic reduction so that a faster route to the nitrosyl complex must be available to account for the observed catalysis. That faster route seems most likely to be the reduction of the coordinated HNO_2 in the $HNO_2Fe^{II}XW_{11}O_{39}^{(n+1)-}$ complex formed in equilibrium (5) of Scheme 4.1, not by electrons originating in the Fe(II) center as in equation. (6), but by the much more energetic electrons available at electrode potentials in the range where the tungsten-oxo framework of the complex is reduced. (The possibility that the HNO_2 might be activated by coordination and become directly reducible at the electrode at the more negative potentials seems

remote because there is little reason for such a direct reduction to follow so closely the variations in the potentials where the tungsten-oxo framework is reduced as the central heteroatom is changed.) Thus, the voltammetry of Figure 4.2C, which cannot be reconciled with an outer-sphere mechanism for the reduction of HNO_2, can be nicely accommodated by Scheme 4.1.

Attempts to measure spectroscopically the rate of reaction (7) in the forward direction by manually mixing NO with the reduced complex were thwarted by the high rate of the reaction. Reaction (7) is written as reversible because the nitrosyl complexes are eventually converted to the original aquo complex when NO is removed from solutions of the complex by extensive bubbling with argon. The observation that the $ONFe^{II}XW_{11}O_{39}^{(n+1)-}$ complexes react with excess NO_2^- can be understood as taking place through the inverse of reaction (7) followed by (5).

The possibility that the NO involved in reaction (7) is generated via reaction (3) instead of reaction (6) could be eliminated because the rate of reaction (3) is too low (17). The apparent preference for HNO_2 over NO_2^- as the oxidant in reaction 6 is not surprising because it avoids the generation of the high energy O^{2-} anion.

The values of k_{obs} measured at pH 5 are listed in Table 4.1. The reaction rate responds to changes in the reducing strength of the heteropolyanion produced by changing the central heteroatom. The stronger reductants appear somewhat more reactive. However, according to Scheme 4.1 the measured values of kobs correspond to the product K_5 k_6 $([H^+]/(Ka + [H^+]))$, where K_5 and k_6 are the equilibrium constant

and rate constant for reactions (5) and (6), respectively, and K_A is the acid dissociation constant of HNO_2. (At pH 5, $k_{obs} = 2 \times 10^{-2} K_5 k_6$). It was not possible to measure K_5 independently, so it remains unclear whether the trend in kobs evident in Table 1 reflects an increase of k_6 or K_5 (or both) with the reducing strength of the heteropolyanion.

Electrochemistry of the $ONFe^{II}XW_{11}O_{39}^{(n+1)-}$ *Complexes.* The peak current for the first, new irreversible, anodic wave obtained in voltammograms for the nitrosyl complexes (Figure 4.5, curve C) corresponds to more than one electron. The position of the wave shifts as the identity of the heteroatom is changed in the same way as the change in the formal potential of the Fe^{III}/Fe^{II} couple in the parent heteropolytungstate. This behavior is consistent with the interpretation of the wave as an essentially iron-based electrode reaction, *i.e.*, the oxidation of Fe(II) to Fe(III), which induces the release and subsequent oxidation of the nitrosyl ligand. The $H_2OFe^{III}XW_{11}O_{39}^{n-}$ ions exhibit no affinity for NO so that its dissociation from the oxidized complex is to be expected and free NO is known to be electro-oxidized at the potentials where the first anodic wave appears (23). Thus, the wave is reasonably assignable to the half-reaction specified in equation. 9.

$$ONFe^{II}XW_{11}O_{39}^{(n+1)-} - 2e^- + H_2O \rightarrow NO_2^- + H_2OFe^{III}XW_{11}O_{39}^{n-} \quad (9)$$

The irreversibility of the first anodic wave is the result of the large positive shift in the potential, where the Fe(II) center is

oxidized when it is coordinated to NO. The $H_2OFe^{III}XW_{11}O_{39}^{n-}$ anion generated during the anodic oxidation is reducible only at much more negative potentials. The large positive shift in the potential where the oxidation of Fe(II) occurs in the $ONFe^{II}XW_{11}O_{39}^{(n+1)-}$ complexes is consistent with substantial back donation of electrons by the Fe(II) center into a π^* orbital of the coordinated NO as was invoked earlier to account for the correlation between the position of the infra-red absorption of the coordinated NO and the reducing power of the Fe(II) center (Table 4.1).

The second anodic wave in curve D of Figure 4.5 appears at the same potential for all four heteropolyanions and corresponds to the potential where NO_2^- is irreversibly oxidized to NO_3^- in separate experiments. The same wave appears whether the nitrosyl complex is prepared by reacting the parent Fe(II) complex with NO_2^- or with NO so that it is clearly associated with the nitrosyl complex itself and not with any residual, unreacted NO_2^- in solution.

Reduction of Coordinated NO. The potential where the catalyzed reduction of the coordinated NO commences in curve E of Figure 4.5 corresponds to the potential of the first, two-electron reduction of the tungsten-oxo framework in the catalyst. The correlation between the two sets of potentials is evident from the values listed in Table 4.3. The potentials of the Fe^{III}/Fe^{II} couples for both the aquo and nitrosyl complexes also shift with the identity of the heteroatom (Table 4.1) but this shift does not correlate as closely with the potentials where the catalyzed reductions of the coordinated NO proceed (Table 4.3). These observations constitute strong

circumstantial evidence that the electrons accepted by the NO group that is bound to the Fe(II) center are delivered via the tungsten-oxo framework and not directly from the electrode. The implication is that the tungsten cage serves as a reservoir for the storage of electrons that are subsequently transferred to the NO group in a concerted, intramolecular, multiple-electron process that is more facile than direct reduction at the electrode. Note that the important fact is not that the catalytic onset occurs at the same potential as the tungsten reductions, which could be simply coincidence, but that the shift in potential of the catalytic onset parallels the shift in the tungsten base reductions and not the iron based reductions. This assertion would be much more difficult to make with confidence were it not for the observed systematic shifts in potential as the identity of the central heteroatom was changed. The ability of the $FeXW_{11}O_{39}^{n-}$ anions to serve as both the site of substrate binding and the source of the reducing electrons evidently contributes to the unique catalytic reactivity patterns that they display. The reason that the electrons that reduce the coordinated NO follow the circuitous route that leads from the electrode to the tungsten-oxo framework and to the iron(II) center before reaching the NO molecule that is the object of their journey can be understood as the result of the back-bonding between the NO and the Fe(II). Unoccupied orbitals on the NO that can accept electrons from the electrode before its coordination to Fe(II) are apparently partially occupied after the coordination and the multiple, empty orbitals available within the tungsten-oxo framework are evidently the most accessible point of entry to the complex for

electrons from the electrode.

Catalyst Durability. To examine the robustness of the catalysts toward repeated cycling under realistic electrolytic conditions, a series of electrolyses were carried out in single compartment cells without separation of the anode and cathode. Large excesses of NO_2^- were added to 0.5 mM solutions of the catalysts. Under these conditions the NO_2^- was consumed both by reaction with the reduced heteropolytungstate generated at the mercury cathode and by oxidation to nitrate at the platinum anode. Presumably the anodic oxidation proceeded both by direct oxidation of NO_2^- and by oxidation of the $ONFe^{II}XW_{11}O_{39}^{(n+1)-}$ nitrosyl complex, whose generation at the cathode (vide supra) was evident from the red color of the solution. Electrolyses were continued until the dark blue color characteristic of the multiply reduced catalysts persisted in the solution to indicate the complete consumption of NO_2^- by reduction and oxidation. At this point, any change in the catalyst concentration was estimated by comparing cyclic voltammetric peak heights with those measured before the electrolyses. No loss of catalyst was detected after 100 electrons per catalyst molecule had been passed, and even with 900 electrons per molecule the loss did not exceed 5% and there was no cyclic voltammetric evidence that new electroactive species had been generated by the repeated cycling. Thus, our initial hope that the entirely inorganic heteropolytungstates would prove to be extremely resistant to oxidative and reductive degradation was realized.

Comparison with the Behavior of Other Catalysts for Nitrite Reduction. The redox chemistry and electrochemistry exhibited by the

$H_2OFe^{III}XW_{11}O_{39}^{n-}$ catalysts in the presence of NO_2^- and NO contrasts with that described recently for water-soluble iron porphyrins (12) and nickel and cobalt cyclam complexes (13) that serve as catalysts for the reduction of NO_2^- and NO and with the behavior of ruthenium and osmium polypyridyl complexes that facilitate stoichiometric reductions of NO_2^- and NO (14). The iron and nickel cyclam catalysts operate at significantly more negative potentials (ca. 1.5 V) than the $H_2OFe^{III}XW_{11}O_{39}^{n-}$ catalysts and the iron porphyrin catalysts yield a different set of reduction products. For example, while hydroxylamine (or its dehydrated equivalent) was found to be a significant side product or an active intermediate in most previous catalytic studies (11-14), the $H_2OFe^{III}SiW_{11}O_{39}^{5-}$ catalysts produced only traces of hydroxylamine even when the electrolyses were stopped near their midpoints where intermediates might have been expected to accumulate. The possibility that the heteropolyanion might also catalyze the reduction of hydroxylamine was ruled out by adding a ten-fold excess of hydroxylamine to a 1 mM solution of the catalyst and noting no change in the cyclic voltammetry of the catalyst (Figure 4.6). Hydroxylamine was also shown to be stable in solutions of the supporting electrolytes and catalysts over time scales comparable to those involved in the electrolyses (ca. 2 hr.).

The redox potentials for the Fe^{III}/Fe^{II} couple in the porphyrins is similar to that in the iron-substituted heteropolytungstates but the two types of complex behave differently toward NO and NO_2^-. The Fe(III) forms of the porphyrins react with NO to form a nitrosyl complex that can be reduced in two one-electron steps (12a). In the

presence of excess NO_2^- and protons, the iron(III) porphyrins are converted to the same reducible nitrosyl complex by reactions with the NO generated by the disproportionation of HNO_2 (12a). By contrast, the $H_2OFe^{III}XW_{11}O_{39}^{n-}$ complexes are unreactive toward both NO and NO_2^-.

The iron(II) forms of the porphyrins react with an excess of NO_2^- in neutral solutions to yield a reduced form of the nitrosyl complex according to unspecified stoichiometry (12). Here, the $H_2OFe^{II}XW_{11}O_{39}^{(n+1)-}$ complexes behave similarly and exhibit the clean stoichiometry (2 Fe^{II} per NO_2^-) expressed in equations. (5) and (7) of Scheme 4.1.

The nitrosyl complexes of the iron porphyrins can apparently exist in three quasi-stable oxidation states separated by one electron and with formal potentials positive of those where the catalytic, dissociative reduction of the nitrosyl ligand proceeds (12). These oxidation states have been depicted as representing iron(II) complexes of NO^+, NO and NO^-. There is no analogous set of stable oxidation states for the $ONFe^{II}XW_{11}O_{39}^{(n+1)-}$ complexes. Oxidation of these complexes leads to dissociation (and subsequent oxidation) of the nitrosyl ligand (Figure 4.5C-D) and their first observable reduction, which occurs at potentials where the tungsten-oxo framework is reduced, results in their destruction with the generation of ammonia (and possibly other reduction products) (Figure 4.5E). In contrast with the iron porphyrins, no ammonia is detected when bulk electrolyses are performed at potentials just negative of the Fe^{III}/Fe^{II} couple.

The greater stability and more extensive set of stable oxidation states for the nitrosyl complexes of the iron porphyrins compared with the iron-substituted heteropoytungstates doubtless reflect the more extensive back bonding that occurs with the former complexes. The difference in back-bonding ability of the Fe(II) centers between the two classes of complexes can also be demonstrated by the relative reactivity toward CO. The $H_2OFe^{II}XW_{11}O_{39}^{(n+1)-}$ complexes show no tendency to bind CO (24) while Fe(II) porphyrins are well-known to do so. The same factor is likely to be the origin of the differences in the pattern of reactivity exhibited by the two classes of complexes during the catalytic reduction of the nitrosyl ligand to lower oxidation states. With the porphyrin complexes, the reducing electrons appear to be added directly to the coordinated nitrosyl ligand with little, if any, participation by other reducible groups such as the methylpyridinium substituents in the iron meso-tetrakis(N-methyl-4 pyridyl) porphyrin (12b). One result is a variety of intermediate reduction products, including hydroxylamine (12). By contrast, the nitrosyl complexes of the iron-substituted heteropolytungstates appear to utilize the reducible tungsten-oxo core to store the reducing electrons temporarily before they are delivered to the unreduced, coordinated nitrosyl ligand in a concerted fashion. Thus, the differences between porphyrins and lacunary heteropolytungstates as ligands for iron(II) lead to significant differences in the outcome of electro-reductions in which they are employed as catalysts.

In biological systems, the six-electron reduction of nitrite to

ammonia is accomplished by the nitrite reductase enzymes (25). It has been demonstrated that the active site in these enzymes is an iron chlorin (26). It has also been observed that there is a separate iron sulfur center present in these enzymes (27) and that electron transfer occurs between the two iron sites (25). It has been recently suggested (12b) that the iron sulfur center may act as an electron reservoir that can deliver electrons to the iron chlorin active site to facilitate the multiple-electron reduction of bound nitrite. The $H_2OFe^{II}XW_{11}O_{39}^{(n+1)-}$ complexes behave in a similar fashion with the tungsten-oxo framework acting like the iron-sulfur electron reservoir and the coordinated iron center acting like the active iron chlorin site in the enzyme. Thus, in a number of respects, the iron-substituted heteropolytungstates act as totally inorganic enzyme mimics.

CONCLUDING REMARKS

The electrocatalytic chemistry we have described for the iron-substituted heteropolytungstates in solutions of nitrite and nitric oxide represents the first example of a durable, entirely inorganic electrocatalyst that exhibits both binding of a substrate and subsequent multiple-electron reduction. The unique pattern of catalytic activity displayed by these transition metal-substituted heteropolyanions, especially their ability to store and deliver multiple electrons to a bound substrate, seems likely to be useful in additional contexts that will hopefully be the subject of continuing investigations.

REFERENCES

1. Toth, J. E.; Anson, F. C., *J. Electroanal. Chem.*, **1988**, *256*, 361.

2. Pope, M.T., Heteropoly and Isopoly Oxometallates, Springer Verlag, Berlin, **1983**, p. 23.

3. Baker, L.C.W.; Baker, V.E.S.; Eriks, K.; Pope, M.T.; Shibata, M.; Rollins, O.W.; Fang, J.H.; Koh, L.L., *J. Am. Chem. Soc.*, **1966**, *88*, 2329.

4. Ref 2, pg. 93.

5. (a) Zonnevijlle, F.; Tourne, C.M.; Tourne, F.T., *Inorg. Chem.*, **1983**, *22*, 1198. (b) Zonnevijlle, F.; Tourne, C.M.; Tourne, F.T., *Inorg. Chem.*, **1982**, *21*, 2751.

6. Weakley, T.J.R., *J. Chem. Soc., Dalton Trans.*, **1973**, 341.

7. Pope, M.T.; Varga, G.M., *Inorg. Chem.*, **1966**, *5*, 1249.

8. McEvoy, A.J.; Gratzel, M., *J. Electroanal. Chem.*, **1986**, *209*, 391.

9. (a) Keita, B.; Nadjo, L., *J. Electroanal. Chem.*, **1988**, *247*, 157. (b) Keita, B.; Nadjo, L.; Saveant, J. M., *J. Electroanal. Chem.*, **1988**, *243*, 105. (c) Keita, B.; Nadjo, L., *J. Electroanal. Chem.*, **1988**, *243*, 87. (d) Keita, B.; Nadjo, L., *J. Electroanal. Chem.*, **1988**, *240*, 325. (e) Keita, B.; Nadjo, L.; Haeussler, J. P., *J. Electroanal. Chem.*, **1987**, *230*, 85. (f) Keita, B.; Nadjo, L., *J. Electroanal Chem.*, **1987**, *227*, 265. (g) Keita B.; Nadjo, L., *J. Electroanal Chem.*, **1986**, *199*, 229. (i) Keita B.; Nadjo, L., *J. Electroanal Chem.*, **1985**, *191*, 441. (j) Keita B.; Nadjo, L., *J. Electroanal Chem.*, **1987**, *230*, 267. (k) Keita B.; Nadjo, L., *J. Electroanal Chem.*, **1987**, *227*, 77. (l) Keita B.; Nadjo, L., *J. Electroanal Chem.*, **1987**, *219*, 355. (m) Keita B.; Nadjo, L., *J. Electroanal Chem.*, **1987**, *217*, 287. (n) Keita B.; Lucas, T.; Nadjo, L., *J. Electroanal Chem.*, **1986**, *208*, 343.

10. Tourne, C.M.; Tourne, F.T.; Malik, S.A.; Weakley, T.J.R., *J. Inorg. Nucl. Chem.*, **1970**, *32*, 3875.

11. Ogura, K.; Ishikawa, H., *J. Chem. Soc. Faraday Tran. 1*, **1984**, *80*, 2243.

12. (a) Barley, M. H.; Takeuchi, K. J.; Meyer, T. J., *J. Am. Chem. Soc.*, **1986**, *108*, 5876. (b) Barley, M. M.; Rhodes, M. R.; Meyer, T. J., *Inorg. Chem.*, **1987**, *26*, 1746.

13. Taniguchi, I.; Nakashima, N.; Matsushita, K.; Yasukouchi, K., *J. Electroanal. Chem.*, **1987**, *224*, 199.

14. (a) Murphy, W. R. Jr.; Takeuchi, K.; Barley, M. H., Inorg Chem., **1986**, *25*, 1041. (b) Murphy, W. R. Jr.; Takeuchi, K. J.; Meyer T. J., *J. Am. Chem. Soc.* **1982,** *104*, 5817. (c) Barley, M. H.; Takeuchi, K. J.; Murphy W. R., Jr.; Meyer, T. J., *J. Chem. Soc., Chem. Commun.* **1985,** 507.

15. Vogel, A., Textbook of Quantitative Inorganic Analysis, 4th ed. Longman House: London, **1983,** p. 356.

16. Snell, L.T. and Snell, F.D., Cororimetric Methods of Analysis, 3rd ed., Vol IV A, Van Nostrand and Co.: New York, **1967**, p. 174.

17. Jolly, W. L., The Inorganic Chemistry of Nitrogen, W. A. Benjamin, Inc.: New York, 1964, p. 78.

18. Ogura, K.; Ozeki, T., *Electrochim Acta*, **1981,** *26*, 877; Ogura, K.; Watanabe, M., *Electrochim Acta*, **1982,** *27*, 111; Ogura, K.; Ishikawa, M., *Electrochim. Acta*, **1983,** *28*, 167.

19. Gans, P.; Sabatini, A.; Sacconi, L., *Coord. Chem. Rev.* **1966,** *1*, 187.

20. In a recent study of the reaction of HNO_2/NO_2^- with Fe^{II}(edta), NO+ was suggested as the reactive form of N(III) at low pH (21). This possibility could be ruled out in the present experiments by the pH independence of the reaction rate at pH < 4.

21. Zang, V.; Kotowski, M.; Van Eldik, R., *Inorg. Chem.*, **1988,** *27*, 3279.

22. Merck Index, Ninth Edition, pg. 6392.

23. Cutta, D.; Landolt, D., *J. Electrochem. Soc.*, **1972,** *119*, 1320.

24. Toth, J.E. and Anson, F. C., unpublished experiments.

25. Losada, M., *J. Mol. Catal.* **1975,** *1*, 245.

26. Murphy, M. J.; Siegel, L. M.; Tove, S. R.; Kamin, M., *Proc. Nat. Acad. Sci. USA*, **1974**, *71*, 612.

27. Aparicio, P. J.; Knaff, D. B.; Malkin, R., *Arch. Biochem. Biophys.* **1975,** *169*, 102.

TABLE 4.1

Correlation of Formal Potentials for

$Fe^{III}XW_{11}O_{39}^{n-}/Fe^{II}XW_{11}O_{39}^{(n+1)-}$ Couples with Their

Spectral and Kinetic Properties

X	E_f [a] mV vs SCCE	ν, [b] cm^{-1}	k_{obs}, [c] $M^{-1}\,s^{-1}$
Si	-210	1710	1.3 ±0.1
Ge	-138	1720	1.0 ±0.1
P	-20	1730	0.6 ±0.1
As	58	1750	0.4 ±0.1

a. Formal potetial measured at pH 5 and 0.1 M ionic strength.

b. Peak in infra-red band assigned to NO stretch in tetra-n-butylammonium salt of $ONFe^{II}XW_{11}O_{39}^{(n+1)-}$

c. Observed 2nd order rate constant for the formation of the nitrosyl complex evaluated at pH 5. The indicated uncertainties are standard deviations for a series of runs at different concentrations of NO_2^-.

TABLE 4.2

Electrolytic Reduction of Nitrite to Ammonia as Catalyzed by Iron-substituted Heteropolytungstates, $Fe^{III}XW_{11}O_{39}^{n-}$ [a]

Expt No.	X [b]	Conc of Catalyst, mM [c]	Sub/cat [d]	Electrons per NO_2^- [e]	Redn. to NH_3, % [f]	Coul Eff., % [g]
1	Si	0.47	40	3.6	21	35
2	Ge	0.45	41	7.7	29	22
3	P	0.46	43	6.4	31	49
4	As	0.44	40	3.8	36	35
5	P	0.47	84	2.6	13	29
6	P	.10	368	1.8	10	33

a. Supporting electrolyte: 0.1 M $CH_3COONa - CH_3COOH$, pH = 4. Stirred mercury pool maintained at -0.9 V. Except for experiment No. 5, electrolyses were halted at the first permanent appearance of the dark blue color characteristic of reduction of the tungsten-oxo framework of the catalysts.

b. Identity of the heteroatom in the catalysts.

c. Initial concentration of catalyst.

d. Ratio of substrate to catalyst.

e. The number of faradays of charge passed per mole of NO_2^- initially present.

f. Percent of the initial NO_2^- converted to NH_4^+ as determined by ion chromatography.

g. Coulombic efficiency for generation of ammonia: (moles of NH_4^+ per faraday of charge) x 6.

TABLE 4.3

Correlation Between the First Reduction Potentials of the Tungsten-oxo Framework and the Potential Where $Fe^{III}XW_{11}O_{39}^{n-}$ Complexes Catalyze the Reduction of NO [a]

X [b]	$-E_f$, [c] mV	$-E_{cat}$, [d] mV
Si	752	760
Ge	725	730
P	702	730
As	690	710

a. $[Fe^{III}XW_{11}O_{39}^{n-}] = [NO_2^-] = 1$ mM; supporting electrolyte: 0.1 M $CH_3COONa - CH_3COOH$, pH = 4. Scan rate = 50 mV/s.
b. Identity of central heteroatom.
c. Formal potential of $Fe^{II}XW_{11}O_{39}^{(n+1)-}/Fe^{II}XW_{11}O_{39}^{(n+3)-}$ couple.
d. Potential where the curent in the presence of NO is 5% larger than the current in its absence.

CHAPTER 5

ELECTROCHEMICAL CHARACTERIZATION OF OTHER TRANSITION METAL SUBSTITUTED HETEROPOLYTUNGSTATES

ELECTROCHEMICAL CHARACTERIZATION OF OTHER TRANSITION METAL SUBSTITUTED HETEROPOLYTUNGSTATES

INTRODUCTION

The major focus of chapters 2 through 4 of this thesis has been on the iron substituted derivatives of the Keggin ions. Although these compounds have shown very interesting electrochemical activity in their own right, it is possible to synthesize a variety of compounds with different transition metals imbedded in the tungsten oxo cage (1). It would be expected that these compounds would also mimic the reactivity of more traditional transition metal compounds, and also retain the excellent durability that has been demonstrated for the iron substituted ions (2). In this chapter the basic electrochemical characteristics of the Mn, Co, Cr, Ni, and Ru derivatized Keggin ions are presented. Initially it was believed that the Mn and possibly the Co substituted derivatives might be interesting catalysts for the reduction of dioxygen and the Ni substituted compounds catalysts for CO_2 reduction. Unfortunately none of these catalytic processes were rapid enough, if they occurred at all, to be useful. It was also believed that the Cr and Ru complexes might be oxidation catalysts, and some preliminary findings are reported here that indicate that they may indeed be of interest for the oxidation of alcohols.

EXPERIMENTAL

Materials. Lacunary derivatives of the Si, P, and Ge centered Keggin ions were synthesized as previously reported (3,4). Transition metal substituted derivatives were synthesized by adding a stochiometric amount of the transition metal of choice either as a solid or in solution, to an aqueous solution of the lacunary derivative (3,4). The transition metal complexes that were employed were: $Mn(ClO_4)_2 \bullet 6H_2O$ (GFS), $Co(ClO_4)_2 \bullet 6H_2O$ (GFS), $Ni(SO_4)_2 \bullet 6H_2O$ (GFS), $Cr(ClO_4)_2$ (prepared by Zn reduction of $Cr(ClO_4)_3 \bullet 6H_2O$ (Alfa)), and $Ru(H_2O)_6$ $(tosylate)_2$ (prepared by Paul Bernhard(5)). The Cr^{II} and Ru^{II} derivatives were prepared under anaerobic conditions to prevent air oxidation of the hexaaquo ions prior to incorporation in the tungsten oxo framework. After incorporation the reduced, complexed ions were air oxidized to their oxygen stable oxidation states, (presumably +3). The compounds were then recrystallized once or twice from water, water/ethanol, or water/ methanol mixtures.

Tetra-n-butyl ammonium (TBA) salts of some of the ions were prepared by addition of TBABr to aqueous solutions of the ions. The presumably mixed TBA^+/H^+ salts precipitated, were collected and recrystallized from CH_3CN. Anhydrous CH_3CN (Burdick and Jackson) for electrochemical experiments was distilled from CaH_2 onto 3Å mol sieves (Linde) and vacuum transfered into the electrochemical cell.

Apparatus and Procedures. Electrochemical measurements were performed with a variety of Princeton Applied Research instrumentation as described previously (2,3). The working electrode for all experiments was glassy carbon (Tokai). Bulk electrolyses were performed at Pt mesh

electrodes (oxidations) or stirred Hg pools (reductions). All potentials for aqueous experiments are reported vs. SSCE, for nonaqueous vs. ferrocene/ferrocinium (Fc/Fc^+, ca. +0.4 V vs. SSCE). Supporting electrolytes for nonaqueous experiments was $TBAPF_6$ (recrystallized twice from ethanol) and for aqueous experiments were the same as listed in other chapters. Uv-vis spectra were recorded on a Hewlett Packard Model # 8450A diode array spectrometer.

RESULTS AND DISCUSSION

Cobalt Derivatives. The cobalt derivatives $Co^{II}SiW_{11}O_{39}^{6-}$ and $Co^{II}PW_{11}O_{39}^{5-}$ could be isolated as the potassium salts and recrystallized as purple crystals from H_2O or H_2O/methanol (6). The formal potential for the Co^{II}/Co^{III} couple of the $CoSiW_{11}O_{39}^{6-}$ ion occurs at about +945 mv at pH=6 and is relatively pH independent (see table 5.1). The Co^{II}/Co^{III} couple for the $CoPW_{11}O_{39}^{5-}$ ion could not be observed before solvent oxidation, even at pH = 6. This result is not that surprising considering that the M^{II}/M^{III} couples of the $MPW_{11}O_{39}^{n-}$ ions are typically > 200 mv more positive than those of the $MSiW_{11}O_{39}^{(n+1)-}$ ions (3,4). Also, an earlier study stated that the $Co^{III}SiW_{11}O_{39}^{5-}$ ion could not be prepared in aqueous solution completely free from the Co^{II} form of the ion, suggesting that even the less powerful oxidant was still potent enough to oxidize H_2O(6).

The purple TBA salts of the $CoPW_{11}O_{39}^{5-}$ ion could be prepared and were soluble in CH_3CN. When dissolved in anhydrous CH_3CN, the H_2O ligand bound to the sixth coordination site of the Co is reported to be replaced by a solvent molecule (7). The CH_3CN-$CoPW_{11}O_{39}^{5-}$ ion

displayed an irreversible oxidation at +0.38 V vs. Fc/Fc^+ (ca. +0.78 V vs SSCE). The irreversibility of this oxidation and its low potential, compared to the aqueous systems, suggest that it is not Co based and possibly involves oxidation of the coordinated CH_3CN. The alternative argument, that the CH_3CN ligand stabilizes the Co^{III} form of the ion by approximately 400 mv compared to the estimated potential with an H_2O or OH^- ligand, does not seem reasonable.

Manganese Derivatives. The pale yellow Mn derivatives of the Si and P based ions could be easily isolated as the K^+ salts (4). Formal potentials of the Mn^{II}/Mn^{III} couples in aqueous solution (see table 5.1) were similar to those previously reported (4). A Bulk electrolysis at a potential more positive of the Mn^{II}/Mn^{III} couple consumed 0.96 e^-/ Mn and resulted in a color change from pale yellow to light red. The Mn^{III} derivatives were stable indefinitely in solution.

The TBA salts of both ions were also prepared. These compounds showed irreversible oxidations in CH_3CN, similar to the Co compounds. Unfortunately, all of the voltammograms of the Mn derivatives, aqueous and non-aqueous, were unaffected by the presence of O_2. This was a disappointing result in light of the report that the tetra-n-hexylammonium Mn^{II} derivatives would reversibly bind O_2 in toluene at low temperature (8). The ability of the Mn^{II} form of the ion to bind O_2 must be due to the absence of any other competing ligand in the toluene solutions.

Chromium Derivatives. Addition of a deoxygenated light blue solution of Cr^{II} to a deoxygenated solution of $SiW_{11}O_{39}^{8-}$ results in a dark

blue solution indicative of reduction of the tungsten oxo framework. This solution can be slowly oxidized to a green solution by air, from which the $Cr^{III}SiW_{11}O_{39}^{5-}$ ion can be isolated and recrystallized (9). At pH 2 no evidence for any Cr based redox activity could be found although the typical pair of $2e^-$ tungsten based reductions were observed (table 5.1). However, at pH 6, evidence for the oxidation of the ion, apparently Cr based, was observed (see figure 5.1). The utility of this compound as an oxidation catalyst at higher pH has yet to be explored. The ions could be interesting oxidation catalysts, especially in light of the well-known uses of high valent Cr compounds in oxidation chemistry.

Nickel Derivatives. The pale green $Ni^{II}SiW_{11}O_{39}^{6-}$ ion could be isolated as the potassium salt and recrystallized from H_2O/MeOH solutions (6). There was no evidence of either an Ni^{II}/Ni^{III} or Ni^{II}/Ni^{I} couple, although a pair 2 electron W framework reductions were apparent (see table 5.1). The fact that the potentials of these reductions were significantly different than those of the lacunary $SiW_{11}O_{39}^{8-}$ ion allowed for the determination that the Ni^{II} cation was indeed bound in the lacuna of the ion. The compounds showed no activity for the reduction of CO_2 in aqueous solution.

Ruthenium Derivatives. The most difficult to characterize, yet perhaps the most interesting of the transition metal substituted derivatives are the ruthenium ions. These ions have not been reported in the literature to date.

A colorless deoxygenated solution of the silicon based lacunary polytungstate turns dark brown immediately on addition of the light

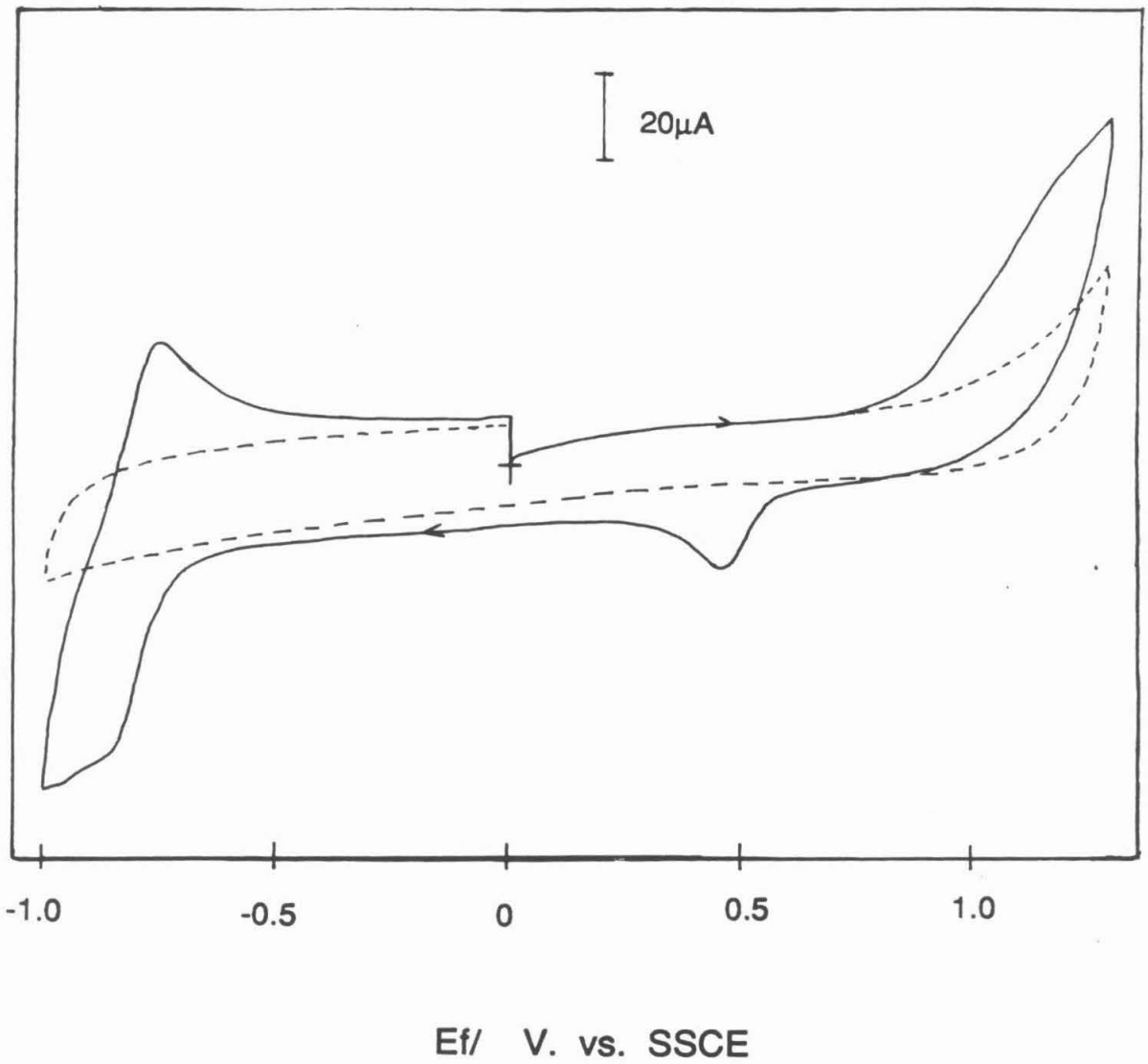

Figure 5.1 Cyclic Voltammograms of backround(- - -)and 1mM. $CrSiW_{11}O_{39}^{-5}$ (——). Supporting electrolyte 0.1 M Na_2PO_4, pH =6, scan rate 50mv/s.

violet $Ru^{II}(H_2O)_6$ ion. A dark brown solid, presumably $H_2ORu^{III}SiW_{11}O_{39}^{5-}$ can be isolated from the solution by addition of KCl followed by ethanol. All cationic Ru based impurities can be removed by passage of the ion down a cation exchange column.

Unfortunately the electrochemistry of the Ru based Si ions is not well defined. At pH 2 several small waves were apparent (see figure 5.2A). Bulk electrolysis at -0.4 V(Hg pool) or +0.6 V (Pt gauze) passed approximately 1 e^- per $Ru^{III}SiW_{11}O_{39}^{5-}$ and resulted in changes in the solution spectra of the ions (figure 5.3). The oxidized form of the ion can (figure 5.3C) also be obtained by addition of H_2O_2 to a solution of the as synthesized ion. The spectra of the reduced ion (figure 5.3B) is oxygen sensitive and exposure to O_2 returns the ion back to the original form (figure 5.3A). The oxygen reduction process is not fast enough to be seen on the cyclic voltammetry time scale. Although it is tempting to assign the +2, +3, and +4 oxidation states to the three forms of the ions, it is unknown if those are the respective oxidation states of the ion. XPS studies of the as synthesized ion (performed by Bruce Tufts) were consistent with the Ru center being in the +3 state. It is unknown at this point whether or not the oxidized form of the ion shows any propensity to dimerize.

The electrochemical response of the $RuSiW_{11}O_{39}$ ion is pH dependent. No electrochemical couple can be observed at pH 6 at glassy carbon or platinum electrodes (figure 5.2B). However, at this higher pH the compound appears to be a catalyst for the electro-oxidation of benzyl alcohol (figure 5.2C). If an excess of benzyl alcohol is added, the catalyst can be turned over several times

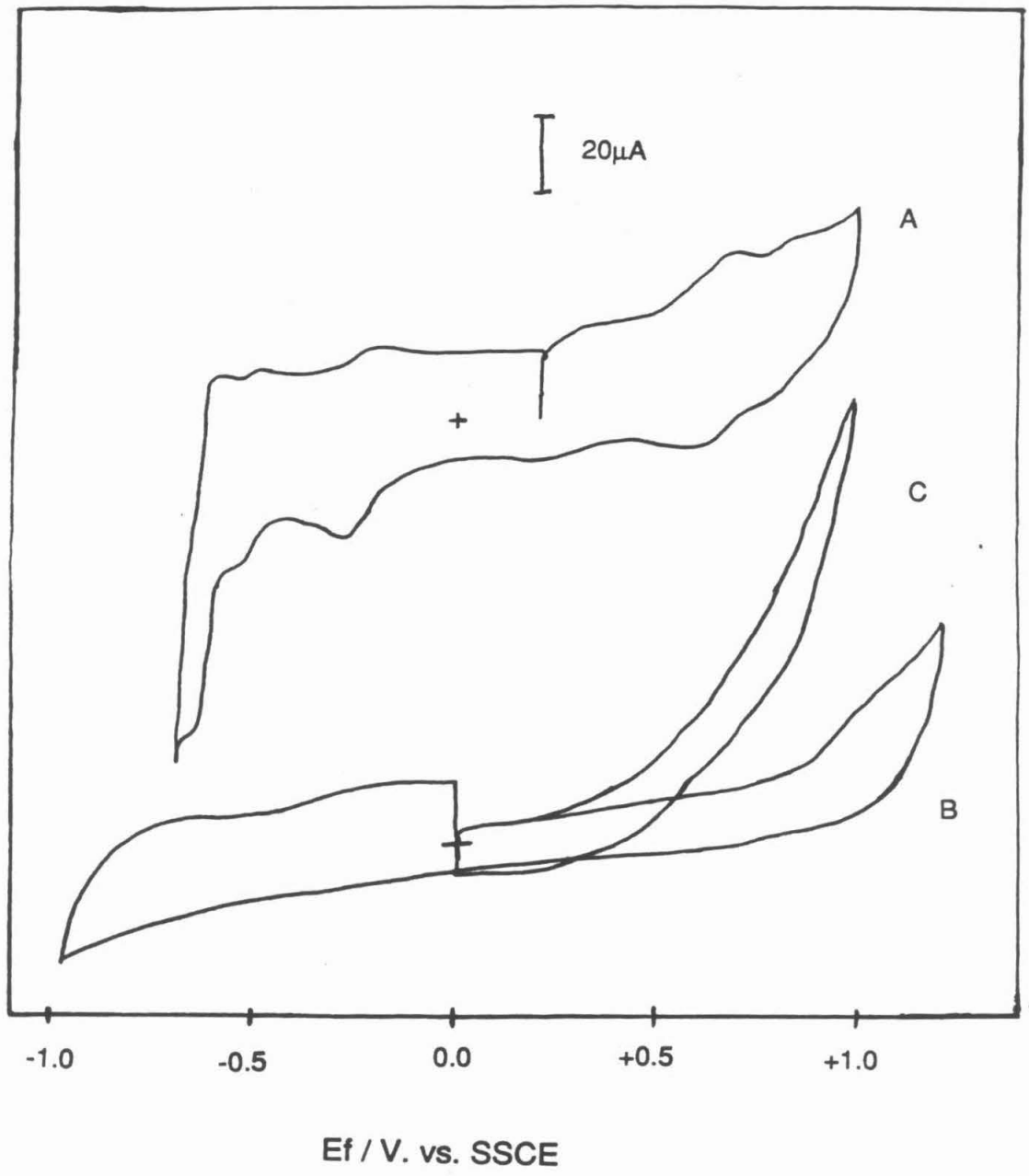

Figure 5.2 Cyclic voltammetry of 1 mM. $RuSiW_{11}O_{39}^{5-}$ at pH=2 (A), pH=6 (B), and in the presence of ca. 10 mM. benzyl alchol at pH = 6 (C). scan rate = 50 mV/sec.

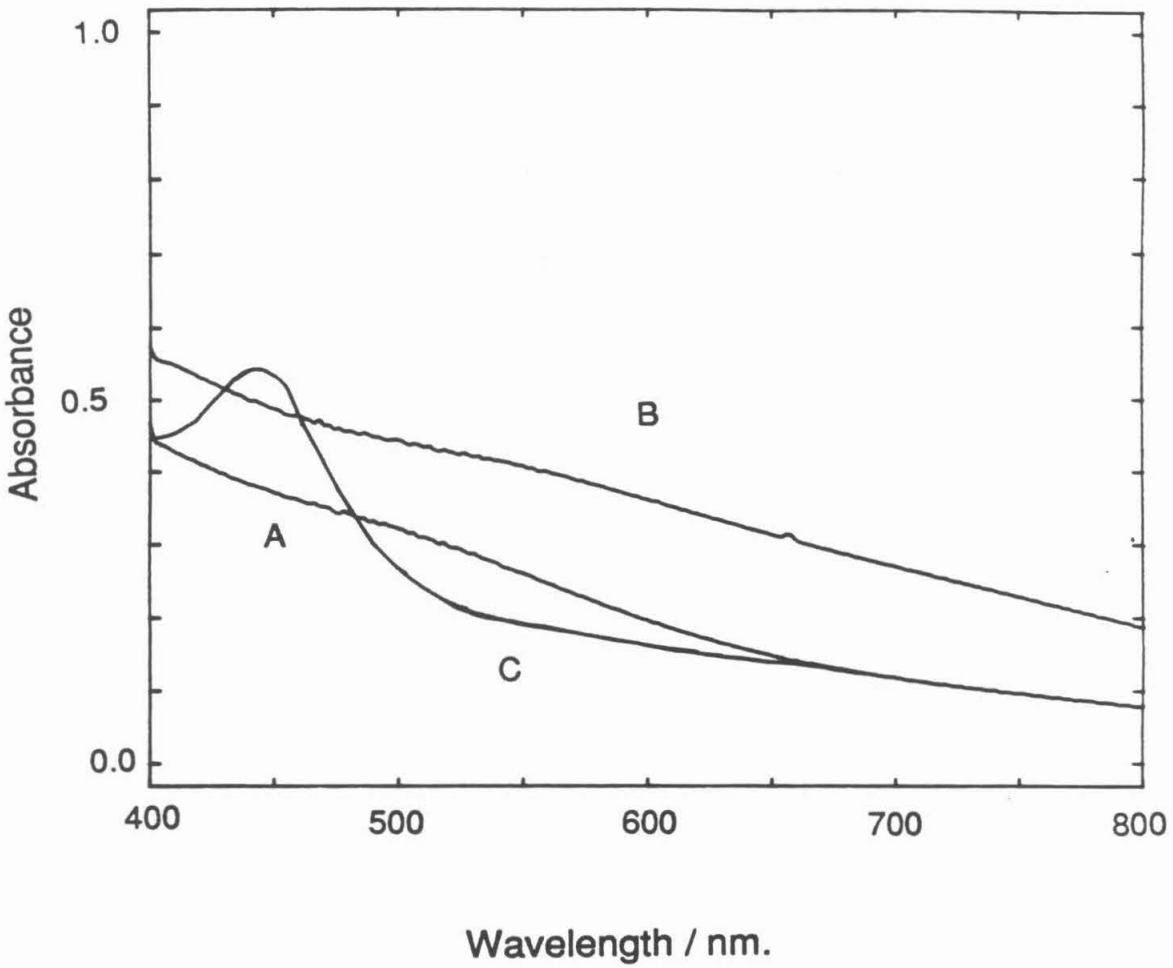

Figure 5.3. Uv-vis spectra of 0.1mM $RuSiW_{11}O_{39}^{5-}$ as synthesized (A), its one electron reduced form(B), and its one electron oxidized form (C). Supporting electrolyte 0.1 M $NaClO_4$.

without any apparent degradation, although the products of the catalysis are still unknown.

CONCLUDING REMARKS

The most promising practical aspect of the electrocatalytic activity of the transition metal substituted heteropolytungstates is their anticipated long term durability, as has been shown in the previous chapter for the reduction of nitrite to ammonia. Both the Cr and Ru based ions would appear to be excellent candidates for studies of electrocatalytic oxidation reactions, processes that are plagued by the durability of typical organo-metallic catalysts. Further study of these compounds should prove extremely interesting.

REFERENCES

1. Pope, M. T., "Heteropoly and Isopoly Oxometallates" Springer-Verlag, Berlin, 1983, p. 59.

2. Toth, J.E.; Anson, F.C.,*J. Am. Chem. Soc.*,**1989**, *111*, 2444.

3. Toth, J.E.; Anson, F.C.,*J. Electroanal. Chem.*,**1988**, *256*, 364.

4. Tourne, C.M.; Tourne, G.F.; Malik, S.A.; Weakley, T.J.R., *J. Inorg. Nucl. Chem.*, **1970**, *32*, 3875.

5. Bernhard, P.; Burgi, H.B.; Hauser, J.; Lehman, H.; Ludi, A.,*Inorg. Chem.*, **1982**, *21*, 3936.

6. Weakley, T.J.R.; Malik, S.A., *J. Inorg. Nucl. Chem.*, **1967**, *29*, 2935.

7. Zonnevijlle, F.; Tourne, C.M.; Tourne, F.T., *Inorg. Chem.*, **1983**, *22*, 1198.

8. Katsoulis, D.E.; Pope, M.T.; *J. Am. Chem. Soc.*, **1984**, *106*, 2327.

9. Katsoulis, D.E.; Pope, M.T.; *J. Chem. Soc. Chem Comm.*, **1986**,, 1186.

TABLE 5.1

Formal Potentials[a] of Redox Couples of Transition Metal Substituted Heteropolytungstates of the General Formula $MXW_{11}O_{39}^{-n}$

M	X	pH	$M^{II/III}$	1st W based[b]	2nd W based[c]
-[d]	Si	2.0	-	-520	-725
-[d]	Si	4.0	-	-632	-830
-[d]	P	2.0	-	-510	-700
Co	Si	2.0	+965	-590	-720
Co	Si	6.0	+945	-	-
Mn	Si	2.0	+470	-550	-
Mn	P	2.0	-	-545	-700
Ni	Si	4.0	-	-698	-822
Ni	Si	2.0	-	-580	-695
Cr	Si	2.0	-	-580	-735
Ru	Si	2.0	-240	-525	-
W	Si	2.0	-	-270[e]	-545[e]

a. Formal potentials of reversible or quasi-reversible waves reported in mV vs. SSCE. Supporting electrolytes buffered at 0.1 M as listed in experimental, Chapter 2.
b. 1st two electron tungsten based wave.
c. 2nd two electron tungsten based wave.
d. lacunary ion.
e. 1 electron wave.